Universidade de Aveiro Departamento de Engenharia Mecânica
2020

**Mafalda
Pereira Gonçalves**

Development of topology optimization methodologies for a modular simulation platform

Desenvolvimento de metodologias de otimização topológica para um software modular de simulação

Universidade de Aveiro Departamento de Engenharia Mecânica
2020

**Mafalda
Pereira Gonçalves**

Development of topology optimization methodologies for a modular simulation platform

Desenvolvimento de metodologias de otimização topológica para um software modular de simulação

Dissertação apresentada à Universidade de Aveiro para cumprimento dos requisitos necessários à obtenção do grau de Mestre em Engenharia Mecânica, realizada sob orientação científica de João Alexandre Dias de Oliveira, Professor Auxiliar, e de Robertt Angelo Fontes Valente, Professor Associado, do Departamento de Engenharia Mecânica da Universidade de Aveiro.

This work was supported by projects UIDB/00481/2020 and UIDP/00481/2020 (Fundação para a Ciência e a Tecnologia, FCT), PTDC/EME-APL/29713/2017 (CENTRO-01-0145-FEDER-029713) and CENTRO-01-0145-FEDER-022083 (Centro Portugal Regional Operational Programme, Centro2020), under the PORTUGAL 2020 Partnership Agreement through the European Regional Development Fund.

o júri / the jury

presidente / president

Prof. Doutor António Gil d'Orey de Andrade Campos
Professor Auxiliar do Departamento de Engenharia Mecânica, Universidade de Aveiro

Doutor João Filipe Moreira Caseiro
Investigador do *CENTIMFE — Centro Tecnológico da Indústria dos Moldes, Ferramentas Especiais e Plásticos*

Prof. Doutor João Alexandre Dias de Oliveira
Professor Auxiliar do Departamento de Engenharia Mecânica, Universidade de Aveiro (orientador)

agradecimentos / acknowledgements

Ao Professor Doutor João Oliveira, pela excelente orientação e pela constante disponibilidade ao longo do último ano. Pelo desafio proposto, pelo conhecimento transmitido e por me incentivar a aprender sempre mais. Um especial obrigada por todo o apoio prestado no decorrer deste trabalho.

Ao Professor Doutor Robertt Valente, pelo constante interesse e disponibilidade demonstrados ao longo deste período. Pelo apoio prestado e pela importante ajuda na reta final deste trabalho.

À Joana, à Beatriz e ao Diogo, por estarem sempre ao meu lado.

Aos meus pais, a quem devo grande parte do que sou hoje. Ensinaram-me a dar sempre o meu melhor e a nunca desistir perante qualquer adversidade.

À minha avó e à restante família que sempre fizeram questão de estar presentes.

Aos restantes amigos e colegas que se cruzaram comigo neste percurso e que viveram comigo as demais aventuras. Os convívios, as noites de festa, os momentos de companheirismo e até os dias passados a estudar. A todos os momentos que jamais esquecerei.

A todos, o meu muito obrigada.

keywords Topology optimization, design-dependent loads, thermoelasticity, software development, MATLAB.

abstract Structural optimization has gained popularity since its first studies in the late 19^{th} century. Over the years, due to the improvement of technology, several works have been focused on its computational implementation. Among the most popular applications, topology optimization deals with the non-homogeneous material distribution in a structure in order to optimize a given structural objective. A compliance approach is usually carried out to evaluate a topology optimization problem. Moreover, it is also considered the Optimality Criterion and SIMP as the optimization method and the material interpolation scheme, respectively.

In this work, several topology optimization problems are carried out and evaluated, from a multi-objective approach, where thermal and mechanical analyses are simultaneously considered, to thermoelastic phenomena. These problems are recognized for incorporating loads that depend on the solution (in this case, thermal loads). Also known as design-dependent loads, they depend on the material layout inside the structure and their magnitude has a direct impact on the optimization process. Therefore, in the resultant topologies, the instabilities associated with this type of loading become evident.

The main focus of this work consists in introducing alternative ways to prevent these issues and deal with the problems' instability. Therefore, an alternative procedure is proposed to control the problems that arise from the mentioned analysis. An adaptation of the Evolutionary Structural Optimization (ESO) method, also known as Bi-directional ESO, is implemented and the obtained results are compared with the conventional ones.

The development of a computational tool consists in an additional outcome of this work and, therefore, the mentioned methodologies are implemented considering a numerical simulation software, based on the Finite Element Method (FEM), as background. Besides the FEM analysis, the computational tool becomes capable of solving different types of topology optimization problems.

palavras-chave

Otimização topológica, carregamentos dependentes da densidade, termoelasticidade, desenvolvimento de *software*, MATLAB.

resumo

A otimização estrutural tem vindo a ganhar popularidade ao longo dos anos e, com o desenvolvimento da tecnologia, tem-se apostado na sua implementação computacional. Uma das áreas de maior desenvolvimento é a otimização topológica. Esta lida com a distribuição não homógenea de material numa estrutura de modo a otimizar um determinado objetivo estrutural. Tendo por base o método mais convencional, a minimização da compliance de uma estrutura é definida como objetivo de um problema de otimização topológica. Para além disso, o Critério do Ótimo, como método de otimização, e o SIMP, como esquema de interpolação do material, são implementados de modo a avaliar o algoritmo.

Neste trabalho, várias abordagens são avaliadas de modo a estudar a aplicação da otimização topológica a problemas muti-física. Uma abordagem multi-objectivo onde as análises térmica e mecânica são simultaneamente ponderadas é estudada, assim como a influência de fenómenos de termoelasticidade. Estes fenómenos são reconhecidos por incorporarem carregamentos que dependem da solução, neste caso, os carregamentos térmicos. Estes são dependentes da distribuição do material na estrutura e a sua magnitude influencia em grande escala o processo de otimização. Nas topologias resultantes, instabilidades associadas a este tipo de carregamentos são notórias e dificilmente contornáveis devido às caraterísticas intrínsecas do processo de otimização escolhido.

No presente trabalho são avaliados os resultados obtidos através dos algoritmos convencionais de otimização topológica. Para além disso, é proposta uma abordagem alternativa de modo a controlar as instabilidades que surgem nas análises referidas e a estabilizar o problema. Uma adapatção do método de otimização estrutural evolucionária (ESO - *Evolutionary Structural Optimization*), conhecida como BESO, é implementada e os resultados obtidos são comparados com os anteriores.

Por fim, um dos resultados deste trabalho consiste no desenvolvimento de uma ferramenta computacional com capacidade para solucionar as abordagens mencionadas. Em conjunto com a análise numérica, baseada no Método dos Elementos Finitos, as metodologias de otimização topológica são implementadas e adicionadas a um software que foi atualizado ao longo deste trabalho.

Contents

List of Tables

Intentionally blank page.

List of Figures

Intentionally blank page.

Chapter 1

Introduction

1.1 Framework

Optimization consists in finding the best solution with the most cost-effective or highest achievable performance under the given constraints. This concept has been widely applied to the most different areas of engineering, from the design of automobile components to the study of water networks. For instance, minimizing the weight of a component or maximizing the efficiency of water equipment are some examples of the application of optimization concepts in real problems [Rao 2009]. These solutions allow the growth of a company's profit and, due to the increased competitiveness, they are now required and expected by companies and customers [A. Campos *et al.* 2015].

Structural Optimization (SO) is the discipline that deals with the optimal design of load-carrying structures taking into account the association between its cost, weight, and stiffness. Different approaches can be established regarding the optimization of a structure, namely the optimization of the overall shape, of a geometrical parameter and of the material layout. Examples of these problems include finding an optimal shape of a suspension arm in a car, an optimal material distribution in the wall of a centrifugal separator, or an optimal cross sectional dimensions of the different beams in a new Eiffel tower [Svanberg 2009]. Nowadays, as a result of technology upgrade, the optimum solutions to these problems can be achieved with the support of computational tools. Such software are capable of analyzing a structure performance under predefined conditions by splitting its domain into discrete parts, also known as "finite elements". Therefore, the Finite Element Method (FEM) is commonly used in numerical optimization as a tool to evaluate the reliability of a structure by computing its displacements and stress fields in order to guarantee suitable solutions.

One of the approaches that has been explored over the years deals with the non-homogeneous material's distribution inside a body. Topology Optimization (TO), the approach explored in this work, is the process of determining the optimum layout of material and connectivity inside a design domain [Deaton and Grandhi 2014]. As a focus of numerous works, its main target consists in strategically distributing the material inside a predefined domain to ensure the structure's maximum stiffness. The conventional method applied to topology optimization is based on the minimization of the structure compliance determined by the work of the external loads. The obtained topologies are achieved by considering the applied loads and the structure's support conditions as well as the results of the numerical analysis. Additionally, the optimum topologies are characterized by the existence of material and void regions. In order to establish the material layout, the Solid Isotropic Material with Penalization (SIMP) method is applied as a material interpolation scheme, being one of the most used in topology optimization problems [Rozvany *et al.* 1992]. According to this approach, the optimization variables are the elements' densities, that can assume any value between 0 and 1, being intermediate densities penalized in order to be avoided in the final topology.

Several works related to topology optimization have already been developed since the fundamental work of Bendsoe and Kikuchi [Bendsøe and Kikuchi 1988]. The greatest part of the existing work focuses on problems where the boundary conditions are independent from the material layout. In contrast to these, problems where the boundary conditions depend on the solution are the main focus of this work. This type of problems might include loads that depend on the existence of material in the structure. For instance, body or thermoelastic stress loads depend on the material distribution inside the domain. This work analyzes thermoelastic stress loads and their impact on the optimization process. The existence of a temperature field on a structure due to heat transfer phenomena is considered along with the thermal loading derived from it. The dependency of thermal loads on the material distribution characterizes them as design-dependent and their effect on the optimum topologies has already been analyzed by numerous authors [Rodrigues and Fernandes 1995, Li *et al.* 1999, Gao and Zhang 2010, Pedersen and Pedersen 2010]. For example, their existence can highly affect the material's behavior and, consequently, the structure's performance [Rodrigues and Fernandes 1995]. Besides, several issues related to their nature appear along the optimization process and studying alternative approaches to overcome these problems is one of the main challenges of this thesis.

Numerical simulation and optimization fundamentals are essential concepts to this work and important know-how of an engineering student. In an academic environment, commercial software is commonly used for learning FEM basis and its optimization toolboxes have been upgraded over the years. These software provide an accessible way of learning important concepts on both subjects. However, to gain detailed knowledge on Finite Element Analysis (FEA) and TO, the implementation of the formulations on code is way more challenging. This Dissertation therefore proposes the development of a computational tool capable of solving different types of topology optimization problems. The background of this work is set on a modular platform, GRIDS Alpha, with a concept that allows further developments by students who are interested in learning more about any of these subjects [Lourenço 2018]. Alongside numerical analyses, this software allows the resolution of topology optimization methodologies.

1.2 Objectives

The main goal of this work is to develop topology optimization strategies capable of solving multi-objective problems. Initially, it is required to implement a topology optimization algorithm to run an elastic and, then, a thermal conduction analysis. Therefore, a multi-objective approach is possible to be carried out by running simultaneously both analyses. The influence of each objective on the optimum solution can be evaluated by pondering the thermal and the mechanical objective-functions.

In addition, with the intention of combining both analyses, a thermoelastic approach to topology optimization is developed. The existence of thermoelastic phenomena on a structure leads to changes in its behavior due to the impact of thermal loads. Therefore, in order to better understand their influence on the optimization process, different approaches to the problem are implemented and carried out. Firstly, the optimization problem is solved by prescribing a uniform temperature field on the structure. Thereafter, instead of the prescribed temperature field, the structure is submitted to thermal boundary conditions, whether they are heat fluxes or prescribed temperatures. The temperature field is then computed by running a thermal analysis according to the material layout. Over the different phases, some problems related to the impact of the thermal loading on the structure's behavior start to come out. These affect the optimization process and, consequently, induce instabilities on the optimum solutions. At this stage, it is necessary to study and implement an alternative method to overcome these issues related to problems where boundary conditions depend on the solution.

Beyond the scientific part, the methodologies implemented in this work will integrate a numerical simulation platform, GRIDS Alpha, developed in MATLAB [Lourenço 2018]. Its features will be enhanced and the developed software will be capable of running several topology optimization methodologies alongside FEM analysis. Developed in a academic environment, it is intended to be an helpful tool for students learning more about both subjects. Also, as an user-friendly and open-source software, this platform presents a modular concept in order to be available to further developments by students or researchers.

1.3 Reading guidelines

This Dissertation is divided into 5 chapters.

- Chapter 1: A general introduction to the work is given, as well as its main objectives;
- Chapter 2: The definitions of the implemented methodologies are presented along with their finite element approximation. Fundamental concepts related to topology optimization are described and, finally, the focus of this work, the treatment of design-dependent loads, is introduced and explored;
- Chapter 3: The global structure of the computational tool is presented alongside the needed implementation details regarding the different developed methodologies;
- Chapter 4: The results obtained for several analyses are presented and analyzed, in order to validate the implemented tool;
- Chapter 5: A global analysis of the work developed is provided as well as some suggestions for future research works.

Intentionally blank page.

Chapter 2

Numerical and mathematical formulation

2.1 Modelling of the thermoelastic behavior

Heat transfer phenomena have to be considered in several problems of different areas of engineering. In this work, the evaluation of these phenomena and, more precisely, thermoelastic ones, is carefully analyzed. The impact of thermoelastic phenomena in the material's behavior has to be taken into account since the existence of temperature variations greatly affects its mechanical behavior. This type of problems consists in the combination of two different ones, such as, the steady-state heat conduction and the linear elasticity. Taking into account linearity assumptions, the definition of the problems is presented. Besides, the application of the Finite Element Method (FEM) helps with a efficient resolution of both problems and, therefore, it is also shown the equilibrium equations of both problems according to a spacial discretization. The formulation shown in this section can be found in more detail in [A. Campos *et al.* 2015].

2.1.1 Linear thermoelasticity

Considering a solid body of volume Ω under small deformations, it is possible to describe a linear elasticity problem by the following equilibrium equation,

$$\mathrm{div}(\boldsymbol{\sigma}) + \mathbf{f} = \mathbf{0}, \tag{2.1}$$

where $\boldsymbol{\sigma}$ stands for the stress field and $\mathbf{f}$ for the load vector that the body is submitted to. The stress field can be computed, taking into account the constitutive law that describes a linear elastic behavior, as

$$\boldsymbol{\sigma} = \mathbf{D} : \boldsymbol{\varepsilon} \quad \text{in} \quad \Omega. \tag{2.2}$$

According to this form of Hooke's law, the linear relation between stress and strain fields can be stated by an elasticity tensor, $\mathbf{D}$. For an isotropic linear material, the elasticity tensor for a two-dimensional plane stress problem turns out to be in the form

$$\mathbf{D} = \frac{E}{(1-\nu^2)} \begin{bmatrix} 1 & \nu & 0 \\ \nu & 1 & 0 \\ 0 & 0 & \frac{(1-\nu)}{2} \end{bmatrix}, \tag{2.3}$$

where ν and E are values that define the material's behavior in the linear range, namely the Poisson's coefficient and the elasticity modulus, respectively. However, the material's mechanical behavior can be affected by the influence of heat transfer phenomena. The existence of temperature variations on the material has to be considered in order to be possible an accurate analysis of its behavior. Therefore, Equation 2.2, that described the linear elastic behavior of a material, must be rewritten as

$$\boldsymbol{\sigma} = \mathbf{D} : \boldsymbol{\varepsilon} - \Delta T \boldsymbol{\beta} \quad \text{in} \quad \Omega, \tag{2.4}$$

where a linear thermoelastic behavior is considered, with $\Delta T \boldsymbol{\beta}$ representing the impact of the temperature differential on the material. This term allows to consider the thermal expansion that the body is submitted to. In addition, the stress field is now dependent on the temperature field, ΔT, and on the thermal properties of the material, $\boldsymbol{\beta}$. Both parameters can be defined as

$$\Delta T = T - T_0, \tag{2.5}$$

$$\boldsymbol{\beta} = \mathbf{D} : \boldsymbol{\alpha}, \tag{2.6}$$

where $\boldsymbol{\alpha}$ represents the vector with the thermal expansion coefficients associated with the different directions and, T_0, the initial temperature of the material. On the other hand, the material deformations, defined by the strain field, $\boldsymbol{\varepsilon}$, can be computed taking into account the displacements field, $\mathbf{u}$, as

$$\boldsymbol{\varepsilon} = \frac{1}{2}\left[\text{grad}(\mathbf{u}) + [\text{grad}(\mathbf{u})]^{\mathrm{T}}\right] \quad \text{in} \quad \Omega. \tag{2.7}$$

The resolution of the problem, namely, the computation of the displacements field, is performed by Equation 2.1. For that purpose, different restrictions have to be established in order to solve the thermoelastic problem. Boundary conditions of Dirichlet and Neumann types are commonly established to restrict and solve these problems. While Dirichlet boundary conditions specify the value that the solution (displacement) must take along the surface Γ_{u}, Neumann boundary conditions will be responsible to specify the values of the derivatives of the solution (that is, the stress) along the surface Γ_σ, by imposing a pre-defined surface load $\bar{\mathbf{t}}$, considering that $\mathbf{n}$ consists in a normal vector to the mentioned surface. Therefore, the specified restrictions can be stated as

$$\mathbf{u} = \bar{\mathbf{u}} \quad \text{in} \quad \Gamma_{\mathrm{u}}, \tag{2.8}$$

$$\sigma \cdot \mathbf{n} = \bar{\mathbf{t}} \quad \text{in} \quad \Gamma_\sigma, \tag{2.9}$$

respectively. Figure 2.1 represents schematically a solid body submitted to thermoelastic boundary conditions, established by Equations 2.8 and 2.9.

Considering the discretization of the domain Ω, the analysis of the thermoelastic problem can be established using the Finite Element Method. According to the domain discretization, the problem can be defined by the following equilibrium equation as

$$\mathbf{K}\mathbf{u} = \mathbf{f}, \tag{2.10}$$

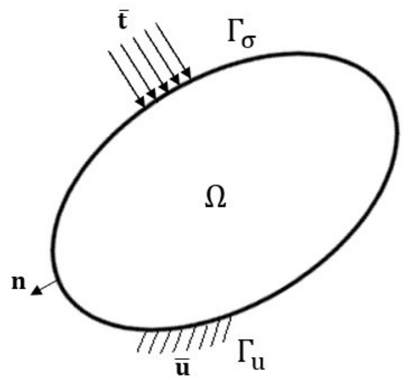

Figure 2.1: Representation of Dirichlet and Neumann boundary conditions applied to a thermoelastic problem.

where $\mathbf{K}$, also defined as global stiffness matrix, consists in the assembly of all the element stiffness matrices taking into account the elements' connectivity. The assembly can be computed by

$$\mathbf{K} = \int_{\Omega} \mathbf{B}^{\mathrm{T}}\mathbf{D}\mathbf{B}\mathrm{d}\Omega, \tag{2.11}$$

where $\mathbf{B}$ matrix includes the shape functions' derivatives. In Equation 2.10, $\mathbf{f}$ stands for the external load vector, which incorporates the load related to thermal expansion, $\mathbf{f}_{\mathrm{th}}$, the vector of distributed loads in surface Γ_σ, $\mathbf{f}_{\mathrm{N}}$, and the n_{T} mechanical nodal loads, $\mathbf{R}_{\mathrm{N}}$, and can be given by

$$\mathbf{f} = \mathbf{f}_{\mathrm{th}} + \mathbf{f}_{\mathrm{N}} + \mathbf{R}_{\mathrm{N}} = \int_{\Omega} \Delta T \mathbf{B}^{\mathrm{T}} \boldsymbol{\beta} \mathrm{d}\Omega + \int_{\Gamma_\sigma} \mathbf{N}_{\Gamma}{}^{\mathrm{T}} \bar{\mathbf{t}} \mathrm{d}\Gamma + \sum_{k=1}^{n_{\mathrm{T}}} (\bar{\mathbf{R}}_{\mathrm{N}})_k. \tag{2.12}$$

2.1.2 Steady-state heat conduction

A steady-state heat conduction problem is defined in a similar way to a linear elasticity one. Although both problems are defined based on different quantities, the equilibrium is stated by the following equation as

$$\mathrm{div}(\mathbf{q}_{\mathrm{k}}) - \mathbf{Q} = \mathbf{0} \quad \text{in} \quad \Omega, \tag{2.13}$$

which describes the heat transfer in a solid body of volume Ω. Only heat transfer by conduction is taken into account, so $\mathbf{q}_{\mathrm{k}}$ stands for superficial fluxes by conduction through its boundary and $\mathbf{Q}$ represents the heat generation inside the body. According to Fourier's law, heat conduction is defined by

$$\mathbf{q}_{\mathrm{k}} = -\mathbf{k} \cdot \mathrm{grad}(\mathbf{T}) \quad \text{in} \quad \Omega, \tag{2.14}$$

where $\mathbf{k}$ represents the thermal conductivity tensor and grad($\mathbf{T}$) stands for the temperature's gradient that the body is submitted to. By replacing Equation 2.14 with 2.13, it is possible to obtain

$$-\mathrm{div}\left[\mathbf{k} \cdot \mathrm{grad}(\mathbf{T})\right] - \mathbf{Q} = 0 \quad \text{in} \quad \Omega. \tag{2.15}$$

In a similar way to the thermoelastic problem, it is necessary to establish boundary conditions in order to solve Equation 2.15. The Dirichlet and Neumann boundary conditions are adjusted for a thermal problem, being defined as

$$T = \bar{T} \quad \text{in} \quad \Gamma_{\mathrm{T}}, \tag{2.16}$$

$$-\bar{q} = [-\mathbf{k} \cdot \mathrm{grad}(\mathbf{T})] \cdot \mathbf{n} \quad \text{in} \quad \Gamma_{\mathrm{q}}, \tag{2.17}$$

respectively. Equation 2.16 establishes a prescribed temperature, $\bar{T}$, in Γ_{T} and the Neumann condition (*vd.* Eq. 2.17) prescribes a superficial flux in surface Γ_{q}, represented by $\bar{\mathrm{q}}$. The mentioned boundary conditions are schematically illustrated in Figure 2.2. Conditions related to convection and radiation, known as Robin's conditions, are not considered in this work.

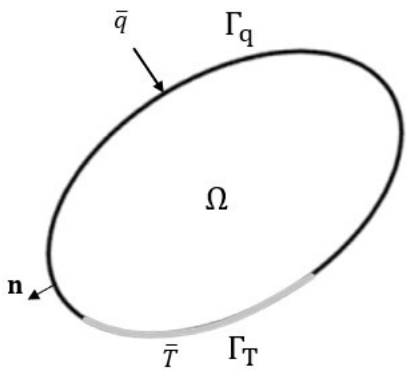

Figure 2.2: Representation of Dirichlet and Neumann boundary conditions applied to a thermal problem.

Proceeding to the domain discretization, the thermal problem can be also solved according to the Finite Element Method. The equilibrium equation that defines the discretized thermal problem can be stated as

$$\mathbf{K}_{\mathrm{T}}\mathbf{T} = \mathbf{q}, \tag{2.18}$$

where $\mathbf{K}_{\mathrm{T}}$ stands for the thermal stiffness, in this case, only related to thermal conductivity, $\mathbf{k}$. In addition, $\mathbf{q}$ represents the nodal fluxes vector, which consists in n_{q} point fluxes, $\bar{\mathbf{P}}_{\mathrm{N}}$. Both quantities can be computed as

$$\mathbf{K}_{\mathrm{T}} = \int_{\Omega} \mathbf{M}^{\mathrm{T}}\mathbf{k}\mathbf{M}\mathrm{d}\Omega, \tag{2.19}$$

$$\mathbf{q} = \sum_{k=1}^{n_{\mathrm{q}}} (\bar{\mathbf{P}}_{\mathrm{N}})_K, \tag{2.20}$$

where $\mathbf{M}$ represents the tensor related to the derivative of the nodal shape functions.

2.2 Structural Optimization

Optimization of any structure or component involves the study of the material's behavior when submitted to different types of loading. The exposure of the material to temperature variations leads to a change in its behavior and, consequently, in the structure's performance. Optimizing the design of a thermoelastic structure consists in an important problem in aeronautics and aerospace products such as turbine engine components and thermal protection systems [Hou *et al.* 2016]. Taking into account the formulation presented in section 2.1, it is possible to estimate the influence of the temperature differential on the structure's performance which makes this knowledge on the subject helpful to the process of optimizing a thermoelastic structure.

In a general way, Structural Optimization (SO) has as its main goal finding the optimum layout of a structure, considering its stiffness, weight and cost. Several studies had already been developed on this topic, but the first one was carried out by Maxwell, who studied different ways of reducing the required material to build a bridge [Maxwell 1870]. According to the obtained results, the optimum structure is composed of discrete elements, whose orientation is similar to the principal directions of the stress field. Therefore, these elements are only subjected to nominal stress since the shear component is considered null. Later on, Michell focused on projecting structures with the minimum material [Michell 1904]. His findings on optimum structures are still used nowadays as analytical benchmarks. One of the most common examples is shown in Figure 2.3, and is known as a Michell *cantilever*.

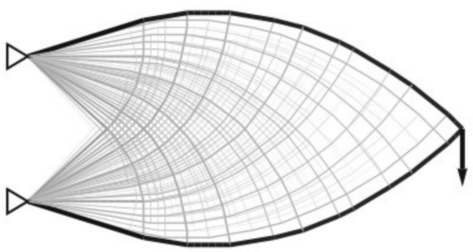

Figure 2.3: Representation of a Michell structure known as Michell *cantilever*. Adapted from [Sokół 2011].

Shape, sizing and topology optimization consist in three different approaches of structural optimization. The first one consists in finding the overall shape of the structure, which maximize or minimize the objective-function. The domain where the problem is established is the design variable, usually defined as the coordinates of relevant points or as geometrical parameters. Sizing optimization, in a similar way to shape optimization, includes structure dimensions as project variables. However, these consist in important parameters that characterize the structure's behavior, whether they are cross-section dimensions or constitutive properties. Finally, Topology Optimization (TO) deals with the connectivity between each point of the structure, which is defined by the design variables, the relative density of each element [A. Campos *et al.* 2015]. In Figure 2.4, it is possible to analyze the different structural optimization categories, where the initial problem is shown (left) along with the optimum solution for the respective approach (right).

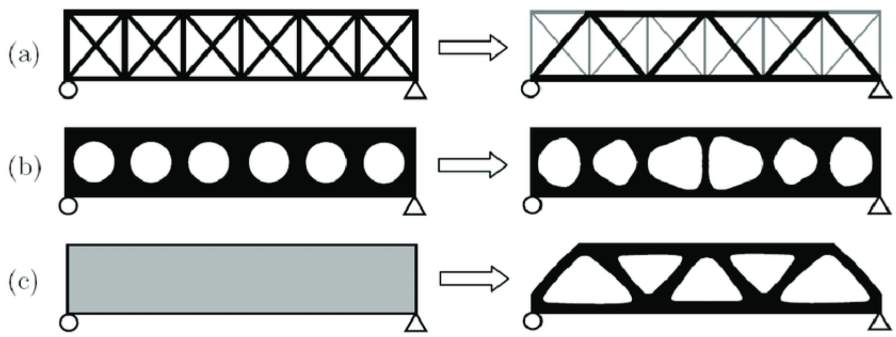

Figure 2.4: Representation of structural optimization categories: (a) sizing optimization, (b) shape optimization and (c) topology optimization. Adapted from [Bendsoe and Sigmund 2003].

As mentioned in the previous chapter, the latter approach (Topology Optimization) was the one chosen for the present work. Topologically optimizing a structure is associated to the material's distribution inside a predefined domain. In the next section, the formulation of the studied problems is presented, as well as some important procedures related to the Topology Optimization algorithm. The optimization concepts and definitions presented in the following sections can be consulted in [A. Campos *et al.* 2015, Bendsoe and Sigmund 2003, Arora 2017].

2.3 Topology Optimization

2.3.1 Overview

Topology optimization of continuum structures has been developed and has become a powerful tool for the design of engineering structures, over the years. Since the fundamental work of Bendsøe and Kikuchi, who presented a material distribution model, based on homogenization methods, several research results have been examined. This study allowed the evaluation of each region of a porous material considering if it was a material or a void one [Bendsøe and Kikuchi 1988]. After the publication of diverse works on the topic, Rodrigues and Fernandes developed a computational model based on the presented material distribution approach [Rodrigues and Fernandes 1995]. It included the effects of temperature differential in the topology design of structures. The work conclusions revealed a strong dependence of the obtained optimum topologies on the temperature differential, even considering a temperature field independent of the design. Therefore, the role of thermal loads and stress in structural analysis and design has been investigated. Significant progress has been made through thermoelastic topology optimization. However, this subject still remains a challenging issue since it belongs to a type of design-dependent problems wherein the thermal stress load changes with the spatial distribution of solid materials [Zhu *et al.* 2019]. This type of loads, also known as design-dependent, are, for example, self-weight loading due to gravity, transmissible or pressure loading, and thermal. In a general way, these refer to loads whose location, direction, or magnitude varies along with changes in the design during the optimization process [Deaton and Grandhi 2014]. As already pointed out, these loads depend on the existence of material on the structure and, during the optimization process, their value changes with the update of the material layout. Diverse research works on this matter have been developed, namely, the different issues that come out when this type of loads are analyzed [Chen and Kikuchi 2001, Bruyneel and Duysinx 2005, Yang *et al.* 2005, Du and Olhoff 2004].

An alternative procedure for the analysis of these problems was studied by Xia and Wang, who applied level-set method to TO of thermoelastic structures [Xia and Wang 2008]. This approach established the free boundary of the structure as a design variable, with the objective-function becoming a function of the structure's shape. The obtained results were compared to the ones from the Solid Isotropic Material with Penalization (SIMP) method, where a large area of gray densities was found. In conclusion, in contrast to SIMP, a black and white design is surely achieved by level-set method. Deng *et. al* explored a topological sensitivity based on the same method to solve two-dimensional stress constrained TO problems subjected to homogeneous temperature change [Deng *et al.* 2014]. The work was extended and a similar approach was applied to large-scale three-dimensional and varying temperature fields [Deng and Suresh 2017]. Using SIMP as an interpolation scheme, Li and Zhang focused on the topology optimization of continuum structures considering a thermomechanical coupling. The minimum strain energy was established as the goal and the adjoint method was used to compute the sensitivities [Li *et al.* 2010]. In regard to the problem's objective-function, Pederson *et al.* explored an alternative approach based on the maximization of the structure's strength, more exactly, on the minimization of the maximum von Mises stress [Pedersen and Pedersen 2010]. The authors defended that compliance may be a questionable objective for the thermoelastic topology optimization problem. Also, Zhang *et al.* addressed the subject by investigating two different minimization objectives, mean compliance and elastic strain energy through sensitivity analysis [Zhang *et al.* 2014]. A concept of load sensitivity was introduced in order to interpret quantitatively the influence of thermal and mechanical loads on the optimum topologies. Since both types of loads present different natures, the two formulations lead to different load sensitivities and, consequently, to different optimal configurations. In order to characterize the dependency of thermal stress loads upon the design variables on multi-phase materials, Gao *et al.* explored penalty models of both the elasticity modulus and the thermal coefficient [Gao and Zhang 2010]. The penalization of only the elasticity modulus can not be applied to those, since the design scheme can only switch between one solid phase and void. Besides, the author also evaluated the use of the Rational Approximation of Material Properties (RAMP) method as an interpolation model, in contrast to SIMP. Under design-dependent loads, SIMP is known to induce the undesirable parasitic effect for low density regions, due to its zero slope at $x = 0$. Therefore, RAMP is found to be effective in overcoming this difficulty, especially for multi-phase material problems. Later on, a stress based formulation was presented by Deaton and Grandhi, with a method for topology optimization of structures with combined mechanical and thermoelastic loads that are subjected to stress constraints [Deaton and Grandhi 2016]. The results indicate that by using the stress-based formulation, structural configurations can be obtained with superior thermal stress performance when compared to those from the minimum compliance formulation. On the other hand, another temperature-constrained topology optimization design method for thermomechanical coupled problems was proposed by Zhu *et al.*. In their work, the temperature values at the heat sources were constrained and the elasticity modulus and the thermal stress were interpolated by the RAMP method [Zhu *et al.* 2019]. Comparing with structures without temperature constraints, this method decreases significantly the temperature and allows the control of the global temperature on the structure. More recently, Kambampati *et al.* presented a level-set topology optimization of structures under coupled mechanical and thermal loads considering stress and temperature constraints [Kambampati *et al.* 2020]. In this work, the conflict between stress and temperature in optimization is evaluated and it is shown that both structural and thermal constraints avoid high values of stress and temperature on the structure, respectively.

2.3.2 Problem definition

Topologically optimizing a structure consists in achieving an optimum solution for the material's layout that maximizes its stiffness or minimizes its compliance (*i.e*, its flexibility). Therefore, it is assumed that the structure is defined in a domain Ω, and sufficiently constrained to ensure its equilibrium. In order to measure the structure's flexibility, it is usually computed its strain energy, S, defined as

$$S = \frac{1}{2}\int_{\Omega} \mathbf{u}^{\mathrm{T}}\mathbf{D}\mathbf{u}\mathrm{d}\Omega, \tag{2.21}$$

where $\mathbf{u}$ stands for the displacements field equivalent to equilibrium. However, an alternative approach to determine the structure's compliance consists in computing the work of the external loads expressed by the following equation,

$$W = \int_{\Omega} \mathbf{f}^{\mathrm{T}}\mathbf{u}\mathrm{d}\Omega, \tag{2.22}$$

where $\mathbf{f}$ represents the external load applied to the structure. Moreover, the total potential energy of the system can also be determined by combining Equations 2.21 and 2.22, as

$$P = S - W, \tag{2.23}$$

which consists in another way to measure the structure's flexibility. This function is minimized by the displacements field $\mathbf{u}$ that corresponds to the structure's equilibrium. According to the minimum total potential energy principle, at the equilibrium, the variation of the total potential energy of the system, P, is equal to zero. Every approach can be used to compute the objective-function. However, the work of the external loads consists in a quantity directly related to the structure's compliance, so this approach is commonly used to evaluate the its flexibility. Therefore, a linear elastic topology optimization problem can be formulated as

$$\begin{aligned} \text{minimize} \quad & \int_{\Omega} \mathbf{f}^{\mathrm{T}}\mathbf{u}\mathrm{d}\Omega = \int_{\Omega} \mathbf{u}^{\mathrm{T}}\mathbf{K}\mathbf{u}\mathrm{d}\Omega, \\ \text{subjected to} \quad & \mathbf{D} \in \mathbf{D}_{\mathrm{adm}}, \\ & \mathbf{K}\mathbf{u} = \mathbf{f}, \end{aligned} \tag{2.24}$$

where $\mathbf{K}$ corresponds to the assembly of all element stiffness matrices. Moreover, as already mentioned in section 2.1, the influence of a temperature differential on the structure has to be taken into account to evaluate the optimization problem in a correct way.

Thermal loads arise from the existence of a temperature field and these need to be considered to the problem's resolution. Accordingly, a thermoelastic topology optimization problem can be formulated in a similar way to the one shown in Equation 2.24. The main difference involves the addition of the thermal loads, $\mathbf{f}_{\mathrm{th}}$, to the loads vector, $\mathbf{f}$, as follows: $\mathbf{f} = \mathbf{f}_{\mathrm{m}} + \mathbf{f}_{\mathrm{th}}$, where $\mathbf{f}_{\mathrm{m}}$ stands for the mechanical loads vector. Consequently, the influence of thermal loads is considered in the structure's equilibrium and, therefore, the displacements in the objective-function already take into account the ones related to the thermal effect. Unlike purely mechanical loads, thermal loads are design-dependent, wherefore the mean compliance ($\frac{1}{2}\mathbf{f}^{\mathrm{T}}\mathbf{u}$) and the elastic strain energy (S) turn out to be inequivalent criteria for this type of problems. The latter one, in contrast to the compliance, does not include the displacements related to thermal expansion. Therefore, both formulations lead to different load sensitivities and, consequently, to different optimum configurations [Zhang *et al.* 2014]. According to Equation 2.12, the thermal loads, $\mathbf{f}_{\mathrm{th}}$, are computed and it is possible to analyze their dependency on the temperature differential applied to the structure, ΔT. The temperature field can be initially prescribed and maintained constant over the optimization process or determined by running a thermal analysis, in each iteration, taking into account the material distribution and the applied thermal boundary conditions.

Alternatively, a thermal problem can also be topologically optimized. Despite the different nature of the involved quantities, the thermal problem can be defined in a similar way to the problem stated in Equation 2.24, related to linear elasticity, with both problems having as their main goal the maximization of a constitutive property. Maximizing the thermal conductivity is the main goal of this type of problem, whereas for the linear elastic problem the objective consists in maximizing the structure's stiffness. Consequently, the thermal problem can be formulated as

$$\begin{aligned} \text{minimize} \quad & \int_{\Omega} \mathbf{T}^{\mathrm{T}}\mathbf{K}_{\mathrm{T}}\mathbf{T}\,\mathrm{d}\Omega, \\ \text{subjected to} \quad & \mathbf{k} \in \mathbf{k}_{\mathrm{adm}}, \\ & \mathbf{K}_{\mathrm{T}}\mathbf{T} = \mathbf{q}. \end{aligned} \tag{2.25}$$

A multi-objective approach can also be established in order to take into account, simultaneously, both objectives, mechanical and thermal, by means of a global objective-function that comprises both. According to a weighted sum, to each objective is associated a weighting coefficient that defines the influence of each analysis. Therefore, it is possible to evaluate the impact of each problem on the optimum solution. The definition of the multi-objective problem can be stated as

$$\begin{aligned} \text{minimize} \quad & \left(\omega_{\mathrm{t}}\frac{f_{\mathrm{t}}}{f_{\mathrm{t}}^{0}} + \omega_{\mathrm{m}}\frac{f_{\mathrm{m}}}{f_{\mathrm{m}}^{0}}\right), \\ \text{subjected to} \quad & \mathbf{D} \in \mathbf{D}_{\mathrm{adm}}, \\ & \mathbf{k}_{\mathrm{T}} \in \mathbf{k}_{\mathrm{adm}}, \\ & \mathbf{K}\mathbf{u} = \mathbf{f}, \\ & \mathbf{K}_{\mathrm{T}}\mathbf{T} = \mathbf{q}, \end{aligned} \tag{2.26}$$

where f_{t} and f_{m} correspond to the thermal and mechanical objective-functions, respectively. The values of the first evaluations of both objective-functions, represented as f_{t}^{0} and f_{m}^{0}, are computed at the first iteration in order to normalize the problem. Both problems present objective-functions of different natures and, therefore, a normalization is required, due to the different values of magnitude that both objective-functions can assume. The impact of each analysis on the obtained results is controlled by the influence given to each one by the respective weighting coefficient, w_{t} and w_{m} (*i.e*, thermal and mechanical influence, respectively), that can be managed through a Pareto analysis.

2.3.3 Solid Isotropic Material with Penalization

A topology optimization problem, regardless of the defined objective-function, is established through a set of project variables. An optimum topology is characterized by the existence of structural and void elements that are described by a design variable, its relative density, ρ. Considering an empty or a material region, its value can be equal to 0 or 1, respectively. However, this definition of the problem leads to the nonexistence of solutions since the continuous introduction of holes will generally decrease the objective function [Sigmund and Petersson 1998]. Relaxing the problem is one of the possible ways to solve this issue and consists in expanding its admissible domain to guarantee the existence of a solution. In 1988, an approach able to deal with this problem was presented by Bendsoe and Kikuchi. Based on homogenization methods, continuum structures were analyzed through multi-scale processes that contributed to an additional detail [Bendsøe and Kikuchi 1988]. Later on, an alternative approach was introduced by Bendsøe, which allowed the relative density of each element, ρ, to vary between the discrete values of 0 and 1, increasing the number of possible solutions [Bendsøe 1989]. Years later, Rozvany et al. focused on this procedure and stated that the intermediate densities should be penalized to achieve a discrete solution for the problem. Therefore, the material properties are defined as the density raised to some power times the properties of a solid material and are considered constant for each element [Rozvany *et al.* 1992]. Also known as "Power-law approach", the Solid Isotropic Material Penalization (SIMP) method is one of the most used ones for topology optimization problems. Its concept can be stated as

$$K = \rho^{p} K_{0}, \tag{2.27}$$

where K_0 corresponds to a base property of the material and p stands for the penalization factor responsible for penalizing the intermediate densities. In Figure 2.5, it is represented the influence of the penalization factor on the effective density of each element. For intermediate values, the density of each element is actually lower, leading to a decrease of the influence on the respective property. Therefore, the extreme values are more beneficial to the optimum solution, being the obtained topology closer to the discrete problem.

Therefore, the problem defined in Equation 2.24 can be rewritten, taking into account the design variable, ρ, as

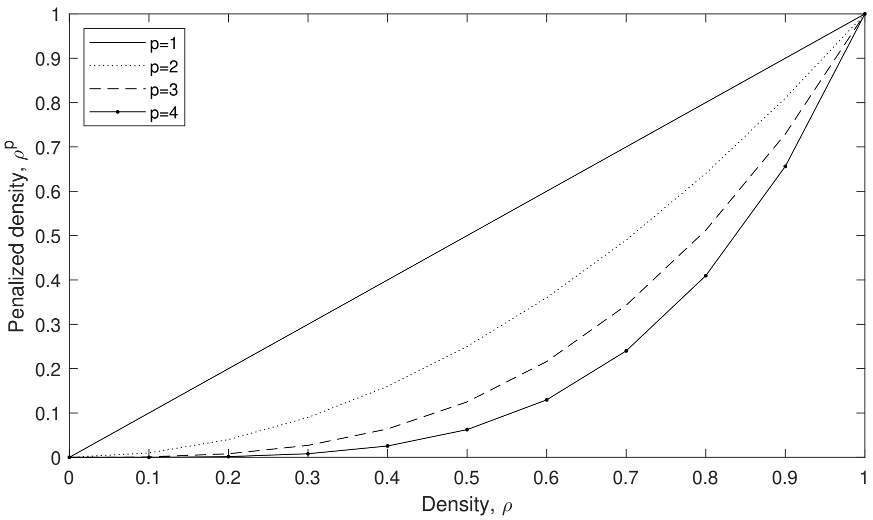

Figure 2.5: Representation of SIMP for different penalties. Adapted from [A. Campos *et al.* 2015].

$$
\begin{aligned}
\text{minimize} \quad & c(\boldsymbol{\rho}) = \int_{\Omega} \mathbf{u}^{\mathrm{T}}\mathbf{K}\mathbf{u}\mathrm{d}\Omega = \sum_{e=1}^{n} \rho_e^p {\mathbf{u}_e}^{\mathrm{T}}\mathbf{k}_0\mathbf{u}_e, \\
\text{subject to} \quad & 0 < \rho_{\min} \leq \rho_i \leq 1, i = 1, ..., n, \\
& \sum_{i=1}^{n} \frac{\rho_i \nu_i}{V_{\Omega}} \leq f_{\mathrm{V}}, \\
& \mathbf{K}\mathbf{u} = \mathbf{f},
\end{aligned}
\tag{2.28}
$$

where $\mathbf{K}$, $\mathbf{u}$, $\mathbf{f}$ stand for the stiffness matrix, displacements and external loads vector, respectively. The element stiffness is defined as $\rho^p\mathbf{k}_0$, where $\mathbf{k}_0$ stands for the stiffness of an element with the base material, f_{V} represents the prescribed volume fraction and ν_i defines the volume of each element. Finally, it is assumed a minimum value, $\rho_{\min}$, for the element relative density in order to avoid singularity issues.

2.3.4 Sensitivity analysis

The sensitivity analysis is crucial for the efficient resolution of a topology optimization problem. The evaluation of the sensitivity provides knowledge on the objective-function's behavior when small changes are applied to the problem's variables. Therefore, the accurate resolution of a topology optimization problem is based on a correct computation of the sensitivity. According to SIMP (*vd.* Sec. 2.3.3), the derivative of the constitutive property, K, relatively to the problem's variable, ρ, can be stated as

$$\frac{\partial K(\rho)}{\partial \rho} = p\rho^{p-1}K_0. \tag{2.29}$$

Considering a discretized version of Equation 2.24, the objective-function, $c(\rho)$, related to a linear elastic problem, can be stated as

$$c(\rho) = \mathbf{f}^{\mathrm{T}}\mathbf{u} = \mathbf{u}^{\mathrm{T}}\mathbf{K}\mathbf{u}. \tag{2.30}$$

Therefore, the sensitivity of the objective-function is defined as

$$\frac{\partial c(\rho)}{\partial \rho} = \mathbf{f}^{\mathrm{T}}\frac{\partial \mathbf{u}}{\partial \rho} + \frac{\partial \mathbf{f}^{\mathrm{T}}}{\partial \rho}\mathbf{u}. \tag{2.31}$$

Considering that $\mathbf{Ku} = \mathbf{f}$ and $\mathbf{K}^{\mathrm{T}} = \mathbf{K}$, it results in $\mathbf{u}^{\mathrm{T}}\mathbf{K} = \mathbf{f}^{\mathrm{T}}$. Based on

$$\frac{\partial \mathbf{f}}{\partial \rho} = \mathbf{K}\frac{\partial \mathbf{u}}{\partial \rho} + \frac{\partial \mathbf{K}}{\partial \rho}\mathbf{u}, \tag{2.32}$$

it is possible to conclude that

$$\frac{\partial c(\rho)}{\partial \rho} = 2\mathbf{u}^{\mathrm{T}}\frac{\partial \mathbf{f}}{\partial \rho} - \mathbf{u}^{\mathrm{T}}\frac{\partial \mathbf{K}^{\mathrm{T}}}{\partial \rho}\mathbf{u}. \tag{2.33}$$

The applied loads in a mechanical problem are independent of the design variable, ρ, so the first term of Equation 2.33 is not considered. Therefore, according to Equation 2.29, the sensitivity of the objective-function, $c(\rho)$, relatively to ρ, results in

$$\frac{\partial c(\rho)}{\partial \rho} = -p\rho_e^{p-1}\mathbf{u}_e^{\mathrm{T}}\mathbf{k}_0\mathbf{u}_e, \tag{2.34}$$

for element e. It is possible to notice that the sensitivity always presents a negative sign due to its definition in terms of the external loads' work. In this case, it is only considered a type of loading that does not depend on the variables of the problem, for example, a mechanical load.

2.3.5 Design-dependent loads

Diverse studies have already been developed in topology optimization problems, considering loads that depend on the problem's variables. This type of loading influences the optimization process as well as the obtained results, so its impact has to be studied and analyzed. Considering the existence of mechanical and thermoelastic loads, $\mathbf{f}_{\mathrm{m}}$ and $\mathbf{f}_{\mathrm{th}}$, respectively, and considering that $\mathbf{f} = \mathbf{f}_{\mathrm{m}} + \mathbf{f}_{\mathrm{th}}$, Equation 2.33 can be rewritten as

$$\frac{\partial c(\rho)}{\partial \rho} = 2\mathbf{u}^{\mathrm{T}}\frac{\partial (\mathbf{f}_{\mathrm{m}} + \mathbf{f}_{\mathrm{th}})}{\partial \rho} - \mathbf{u}^{\mathrm{T}}\frac{\partial \mathbf{K}^{\mathrm{T}}}{\partial \rho}\mathbf{u}. \tag{2.35}$$

Thermoelastic loads derive from the existence of a temperature field on the structure due to heat transfer phenomena. Since they depend on the existence and distribution of the material on the domain, their value is always changing over the optimization process. Therefore, their dependency on the design variables has to be considered. The term related to the thermal loads, $\mathbf{f}_{\mathrm{th}}$, in Equation 2.12, can be adapted for the optimization problem as

$$\mathbf{f}_{\mathrm{th}} = \int_{\Omega_e} \Delta T \mathbf{B}^{\mathrm{T}} \boldsymbol{\beta}(\rho) \mathrm{d}\Omega. \tag{2.36}$$

Considering a one solid material and void distribution, it is possible to penalize only the elasticity modulus in the thermal load stress, regardless of the thermal expansion coefficient, $\boldsymbol{\alpha}$ [Gao and Zhang 2010]. Consequently, $\boldsymbol{\beta}$ can be defined as

$$\boldsymbol{\beta}_e = \boldsymbol{\beta}(\rho) = \mathbf{D}(\rho) : \boldsymbol{\alpha} = ({\rho_e}^p \mathbf{D}^0) : \boldsymbol{\alpha} = {\rho_e}^p \boldsymbol{\beta}^0, \tag{2.37}$$

which allows to rewrite Equation 2.36 as

$$\mathbf{f}_{\mathrm{th}}{}^e = {\rho_e}^p \int_{\Omega_e} \Delta T \mathbf{B}^{\mathrm{T}} \boldsymbol{\beta}_0 \mathrm{d}\Omega = {\rho_e}^p \mathbf{f}_{\mathrm{th}_0}{}^e, \tag{2.38}$$

where $\mathbf{f}_{\mathrm{th}_0}{}^e$, the thermal loads vector related to the material's homogeneous distribution, can be defined as

$$\mathbf{f}_{\mathrm{th}_0}{}^e = \int_{\Omega_e} \Delta T \mathbf{B}^{\mathrm{T}} \boldsymbol{\beta}_0 \mathrm{d}\Omega. \tag{2.39}$$

Therefore, the sensitivity of thermal load stress relatively to the element's relative density, ρ, can be computed by

$$\frac{\partial \mathbf{f}_{\mathrm{th}}{}^e}{\partial \rho} = p {\rho_e}^{p-1} \mathbf{f}_{\mathrm{th}0}{}^e, \tag{2.40}$$

which is assumed valid considering a uniform temperature variation temperature variation on the structure. Finally, the sensitivity of the objective-function, for thermoelastic stress loads, can be expressed by

$$\frac{\partial c(\rho)}{\partial \rho} = 2p {\rho_e}^{p-1} {\mathbf{u}_e}^{\mathrm{T}} \mathbf{f}_{\mathrm{th}0}{}^e - p {\rho_e}^{p-1} {\mathbf{u}_e}^{\mathrm{T}} \mathbf{k}_0 \mathbf{u}_e. \tag{2.41}$$

In contrast to Equation 2.34, which represents a negative sensitivity, this one presents two terms with opposite signs. While the first is only related to design-independent loads, Equation 2.41 refers to a problem with both types of loads. It is possible to analyze the opposite sign of both terms and, depending on the magnitude of each one, the sensitivity can switch between signals along the iterative process. Therefore, the objective-function monotony is interrupted and the problem's convergence is affected. Consequently, several issues start to appear associated with this type of loads.

2.3.6 Optimality Criterion

Optimality criterion is a gradient-based method widely used for problems in which the number of restrictions is lower than the number of variables [Bendsoe and Sigmund 2003]. Its application in structural analyses was introduced by Prager by establishing an optimality criterion for structural design [Prager 1968]. Nowadays, its application is widespread in topology optimization problems and its main objective consists in updating the variables that define the structure based on an optimum criterion. A generic optimization problem can be defined as

$$\begin{aligned} \text{minimize} \quad & c(\mathbf{x}), \\ \text{subjected to} \quad & g(\mathbf{x}) = 0, \end{aligned} \tag{2.42}$$

where the stationary condition is established, based on the Karush–Kuhn–Tucker (KKT) conditions, by

$$\Delta c\left(\mathbf{x}^*\right) + \lambda^{*\mathrm{T}} \Delta g\left(\mathbf{x}^*\right) = \mathbf{0}. \tag{2.43}$$

Considering a problem with only one restriction, g, Equation 2.43 can be rewritten as

$$-\frac{\partial c}{\partial x_i} = \lambda \frac{\partial g}{\partial x_i}, \tag{2.44}$$

where λ stands for the Lagrange multiplier that is defined as

$$\lambda = -\frac{\frac{\partial c}{\partial x_i}}{\frac{\partial g}{\partial x_i}}. \tag{2.45}$$

The Lagrange multiplier evaluates how the variable x_i affects the restriction g, and its value is constant in the whole domain at the optimum point. Based on the presented equations and considering a fixed point iteration scheme, the variable's update can be established by

$$x_i^{(k+1)} = x_i^{(k)} \left(-\frac{\frac{\partial c}{\partial x_i}}{\lambda \frac{\partial g}{\partial x_i}} \right)^{\frac{1}{\gamma}}, \tag{2.46}$$

where γ is responsible for controlling the step of each iteration k. A lower value results in higher updates in variables, although, it can lead to convergence problems. Based on an heuristic approach, the optimality criterion can be applied to a topology optimization problem as

$$\rho_e^{\text{new}} = \begin{cases} \max(\rho_{\min}, \rho_e - m) \\ \quad \text{if } \rho_e \beta_e^{\eta} \leq \max(\rho_{\min}, \rho_e - m), \\ \rho_e \beta_e^{\eta} \\ \quad \text{if } \max(\rho_{\min}, \rho_e - m) < \rho_e \beta_e^{\eta} < \min(1, \rho_e + m), \\ \min(1, \rho_e + m) \\ \quad \text{if } \min(1, \rho_e + m) \leq \rho_e \beta_e^{\eta}, \end{cases} \tag{2.47}$$

where m is a positive move-limit parameter, μ is a numerical dumping coefficient, and B_e is a parameter found by the optimality condition, stated as

$$B_e = \frac{\frac{-\partial c}{\partial \rho_e}}{\lambda \frac{\partial V}{\partial \rho_e}}. \tag{2.48}$$

The Lagrange multiplier, λ, also needs to be updated over the optimization process in order to accomplish the volume restriction. Based on a bi-sectioning method, its value can be computed by

$$g(\lambda) = V(\rho(\lambda)) - f_{\mathrm{V}} \bar{V}. \tag{2.49}$$

In Figure 2.6, it is illustrated, in a schematic way, the iterative process responsible for updating the Lagrange multiplier in each iteration.

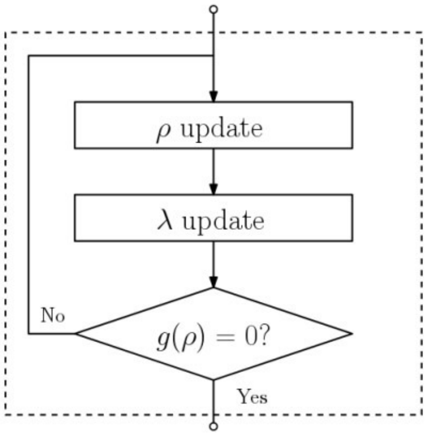

Figure 2.6: Representation of the iterative process inside Optimality Criterion. Adapted from [A. Campos *et al.* 2015].

The convergence of both the iterative cycle and the optimization problem is established when, for all the intermediate densities, $B_e = 1$ and, consequently, $\rho^{k+1} = \rho^k$.

2.3.7 Bi-directional Evolutionary Structural Optimization

A topology optimization problem is usually solved in a conventional way by applying gradient-based search methods, such as, for example, the Optimality Criterion. This consists in an iterative approach where the same calculations are repeated in each and every iteration. An initial design is estimated and improved in each iteration, until optimality conditions are satisfied. Alternatively, there are also algorithms inspired by natural phenomena, also known as Nature-inspired methods, for example, the Genetic Algorithms (GA). These, by contrast, do not require the continuity or differentiability of the problems' functions, wherefore stochastic ideas and random numbers generation are used to search for the optimum point. The application of these algorithms to structural optimization, more precisely, to topology optimization has already been the focus of several works. However, these methods require a large amount of function's evaluations to analyze a topology optimization problem leading to a prohibitive computational effort [Arora 2017]. In this work, an evolutionary algorithm, known as Evolutionary Structural Optimization (ESO) method, is applied to the optimum design of a structure. This method began as a non-gradient based algorithm and has gained widespread popularity among researches in structural optimization. Firstly used by Xie and Steven in structural optimization, its main idea relies on having a continuously evolving design, that slowly improves until it reaches the optimum [Xie and Steven 1993]. Several developments have already been made on the original method, so evolutionary algorithms began to adopt gradient-based techniques, such as the sensitivity number to determine which elements to remove [Munk *et al.* 2015]. Therefore, its original idea relies on an empirical concept that the structure evolves towards an optimum by slowly removing elements with lowest sensitivity numbers [Huang and Xie 2010].

This method has already been applied to diverse works on topology optimization and its effectiveness has been proved. Furthermore, its application on problems with design-dependent loads has also been performed. Regarding this type of problems, Li *et al.* focused on the study of topology optimization of thermoelastic structures with displacement minimization [Li *et al.* 1999]. Years later, the same algorithm was applied to topology designs involving varying temperature fields due to heat transfer phenomena [Li *et al.* 2001a]. A latter work developed by the same authors extends the ESO algorithm to optimum topology designs of thermoelastic structures subjected to various complex thermal environments [Li *et al.* 2001b]. An extension of the presented method was developed by Querin *et al.*. Known as Bi-directional ESO (BESO), its main idea relies on adding new elements to the structure in the locations next to those with highest sensitivity numbers apart from the idea of removing the less efficient ones [Querin *et al.* 1998]. In a similar way to ESO, this method was also evaluated in topology optimization problems and its results were proved to be similar to the ones from the conventional method. However, the study of design-dependent loads was also performed by BESO method in the subsequent years. Focused on the study of design-dependent self-weight loads, Huang and Xie proposes a new BESO method using an alternative material interpolation to SIMP [Huang and Xie 2011]. Regarding the same type of loading, a efficient sensitivity computation was proposed by Rubén Ansola *et al.*. To enhance the convergence of the algorithm in order to achieve the optimum design, a correction factor was suggested to compute the sensitivities [Ansola *et al.* 2006]. Besides, Yang et al. proposes a modification of the sensitivity number in order to accommodate transmissible loads, surface loading with fixed load direction, and self-weight body loads in the conventional BESO procedure [Yang *et al.* 2005]. According to the formulation applied to the previous problems, and according to the BESO algorithm, a topology optimization problem can be stated as

$$\begin{aligned} \text{minimize} \quad & c = \int_{\Omega} \frac{1}{2}\mathbf{f}^{\mathrm{T}}\mathbf{u}\,\mathrm{d}\Omega, \\ \text{subjected to} \quad & \rho_i \in \{\rho_{\min}, 1\},\ i = 1, ..., n, \\ & \sum_{i=1}^{n} \frac{\rho_i \nu_i}{V_{\Omega}} \leq f_{\mathrm{V}}, \\ & \mathbf{K}\mathbf{u} = \mathbf{f}, \end{aligned} \tag{2.50}$$

where $\mathbf{f}$ and $\mathbf{u}$ correspond to the loads and displacements vector, respectively. The loads vector takes into account the applied mechanical load, $\mathbf{f}_{\mathrm{m}}$, and the thermal loads, $\mathbf{f}_{\mathrm{th}}$, that the structure is subjected to. In addition, the objective-function, c, consists in the mean compliance instead of the compliance used in the conventional method (*vd.* Eq. 2.50).

According to the main idea of this method, it is necessary to establish a ranking of sensitivity numbers in order to understand which elements should be added or removed. Concerning the sensitivity numbers for solid elements, these can easily be estimated by the approximate variation of the objective-function due to the removal of these individuals elements. By contrast, for void elements, these are harder to determine. Consequently, the addition of new elements is performed in the neighborhood of the elements with higher sensitivity numbers. Besides, Huang and Xie proposed a new BESO approach based on SIMP. In a similar way to the conventional method, based on the sensitivity analysis, a definition of the sensitivity number is presented using a penalty parameter [Huang and Xie 2009]. Taking into account the existence of design-dependent loads, Yang et al. proposed a modified sensitivity number in order to include the influence of design-dependent loads on the optimization process [Yang *et al.* 2005]. Therefore, the sensitivity of the objective-function can be computed in a similar way to section 2.3.5. Considering the mean compliance ($\frac{1}{2}\mathbf{f}^{\mathrm{T}}\mathbf{u}$) as the objective-function, the sensitivity can be given by

$$\frac{\partial c(\rho)}{\partial \rho} = p{\rho_e}^{p-1}{\mathbf{u}_e}^{\mathrm{T}}{\mathbf{f}_{\mathrm{th}_0}}^{e} - \frac{1}{2}p{\rho_e}^{p-1}{\mathbf{u}_e}^{\mathrm{T}}\mathbf{k}_0\mathbf{u}_e, \tag{2.51}$$

where ${\mathbf{f}_{\mathrm{th}_0}}^{e}$ stands for the thermal loads computed initially for the material's homogeneous distribution. However, if a thermal analysis is carried out to update the temperature field, this quantity is given by $\mathbf{f}_{\mathrm{th}}$ and has to be computed in each iteration. As mentioned, the BESO method establishes a "black and white" topology for which reason the design variables can only assume discrete values. Therefore, according to the SIMP method, the sensitivity number can be stated as

$$\alpha_i = \frac{-1}{p}\frac{\partial c}{\partial \rho_i} = \begin{cases} \frac{1}{2}\mathbf{u}^{\mathrm{T}}\mathbf{K}\mathbf{u} - \mathbf{u}^{\mathrm{T}}{\mathbf{f}_{\mathrm{th}}}^{0} & \text{when } \rho_i = 1 \\ \frac{{\rho_i}^{p-1}}{2}\mathbf{u}^{\mathrm{T}}\mathbf{K}\mathbf{u} - {\rho_i}^{p-1}\mathbf{u}^{\mathrm{T}}{\mathbf{f}_{\mathrm{th}}}^{0} & \text{when } \rho_i = \rho_{\mathrm{min}} \end{cases}. \tag{2.52}$$

In contrast to the sensitivity number for material elements, the one that corresponds to void elements is dependent on the penalization factor. Alternatively, assuming that the penalty is equal to infinity, the sensitivity number can be rewritten as

$$\alpha_i = \frac{-1}{p}\frac{\partial c}{\partial \rho_i} = \begin{cases} \frac{1}{2}\mathbf{u}^{\mathrm{T}}\mathbf{K}\mathbf{u} - \mathbf{u}^{\mathrm{T}}{\mathbf{f}_{\mathrm{th}}}^{0} & \text{when } \rho_i = 1 \\ 0 & \text{when } \rho_i = \rho_{\mathrm{min}} \end{cases}. \tag{2.53}$$

The approach mentioned in Equation 2.53 is similar to the original BESO method, also known as "hard-kill" approach. It is noticeable that considering the penalty factor equal to infinity, the original "hard-kill" method turns out to be a special case of the new approach, known as "soft-kill" BESO. Moreover, in both approaches, the sensitivity numbers are computed based on different status of elements (ρ_{min} and 1), so there could be difficulties in the convergence of the objective-function and also in the corresponding topology. An effective way to avoid this problem consists in averaging the sensitivity number with its historical information [Huang and Xie 2007]. Consequently, the new sensitivity number can be expressed by

$$\alpha_i = \frac{1}{2}\left(\alpha_{i,k} + \alpha_{i,k-1}\right), \tag{2.54}$$

where k represents the number of the current iteration.

2.3.8 Control of stability

In topology optimization problems, different numerical issues appear commonly in the obtained results. These can be divided into three categories, such as, checkerboards, mesh-dependence and local minima. The first ones consist in the appearance of regions of alternating solid and void elements. On the other hand, mesh-dependency phenomena refer to obtaining different qualitative solutions for different discretizations and mesh sizes. Finally, the last one is characterized by obtaining different solutions to the same discretized problem when choosing different starting solutions [Sigmund and Petersson 1998].

Several techniques are used to ensure the existence of solutions in a topology optimization problem and also to avoid the existence of the mentioned numerical issues. One of them consists in a filtering technique that is also used to restrict the problem. Known as checkerboard filter, this technique, introduced by Sigmund, is based on filtering techniques from image processing. This filter modifies the sensitivities, computed by Equation 2.34, taking into account a weighted average of the element sensitivities in a fixed neighborhood. Despite the purely heuristic principle of this filter, it produces similar results to local gradient constrained ones with a simpler implementation [Sigmund and Petersson 1998]. Therefore, according to Equation 2.55, the new sensitivity of element e is dependent on the sensitivities of elements in a predefined neighborhood and can be determined by

$$\frac{\partial c}{\partial \rho_e} = \frac{1}{\frac{\rho_e}{v_e}\sum_{i \in N_e} H_i} \sum_{i \in N_e} H_i \rho_i \frac{\partial c}{\partial \rho_i}, \tag{2.55}$$

where H_i, the convolution operator, defined as

$$\begin{gathered} H = r_{\min} - \operatorname{dist}(e,f), \\ f \in N \mid \operatorname{dist}(e,f) \leq r_{\min}, e = 1,..,N, \end{gathered} \tag{2.56}$$

which allows the evaluation of the weight of each element in the new sensitivity of element e. The convolution operator is computed considering the distance between the centers of each element, e and f, and the predefined radius of the filter area, $r_{\min}$. Only the elements inside the filter area are taken into account and their influence on the sensitivity of element e linearly decreases with the distance between them and element e. Therefore, the sensitivity converges to the original one when the radius approaches zero and all sensitivities will be equal when $r_{\min}$ approaches infinity [Sigmund and Petersson 1998]. Outside the filter area, the operator H is considered null. Finally, the modified sensitivities are used by the optimization algorithm to update the design variables.

In contrast to the conventional method, the evolutionary structural optimization method presents a different operating mode. Instead of searching for an optimum solution since the beginning of the process, the structure evolves to one with the required volume and, then, to an optimum solution. Apart from that, a checkerboard filter is also applied to the BESO method in order to avoid the same numerical instabilities [Huang and Xie 2010]. In this method, the sensitivity numbers computed by Equations 2.52 and 2.53 reflect the efficiency of each element on the structure's compliance without carrying any physical meaning. The applied filter is rather similar to the one used in SIMP method.

In a similar way, the sensitivity numbers are defined by averaging those of the connected elements in a established neighbourhood. Initially, the neighbourhood is defined by the parameter $r_{\min}$ that consists in the radius of a circle centered on the centroid of element e. Only the nodes located inside the defined circle contribute to the new sensitivity number of element e. Therefore, through the computation of a weight factor as

$$\omega\left(r_{e,f}\right) = \begin{cases} r_{\min} - r_{e,f} & \text{for } r_{e,f} < r_{\min} \\ 0 & \text{for } r_{e,f} \geq r_{\min} \end{cases}, \tag{2.57}$$

it is possible to determine the influence of the neighboring elements on the sensitivity number of element e. Taking this into account, the modified sensitivity number is stated as

$$\hat{\alpha}_e = \frac{\sum_{f=1}^{N_e} \omega\left(r_{e,f}\right) {\alpha_f}^n}{\sum_{f=1}^{N_e} \omega\left(r_{e,f}\right)}, \tag{2.58}$$

where N_e is the total number of nodes in the neighbourhood and $r_{e,f}$ denotes the distance between the center of the elements e and f. It is possible to verify that the sensitivity numbers for void elements are provided by filtering the sensitivity numbers of their neighboring solid elements.

Intentionally blank page.

Chapter 3

Software Architecture and Implementation

3.1 Overview

One of the objectives of this dissertation consists in the development of a computational tool capable of solving different topology optimization problems. Several procedures based on linear elasticity and thermal conduction are developed, such as, a multi-objective approach and a thermoelastic analysis. A numerical simulation software, already implemented in MATLAB, is the basis for the integration of the developed methodologies.

GRIDS Alpha was developed by Rúben Lourenço as an outcome of his Master's Thesis [Lourenço 2018]. Developed in an academic environment, its main objective was to be a helpful tool for students and researchers. Additionally, it also allows further developments by the integration of new modules. The upgrade of its functionalities by the addition of new features developed by other students is consistent with its open-source and modular concepts. Thereby, students can develop a deeper understanding on numerical simulation concepts when dealing with the code's implementation themselves.

The features of the original software consist in numerical analysis of two-dimensional problems according to different finite element formulations. As a Finite Element Analysis (FEA) platform and taking advantage from its modular concept, this work proposes an upgrade of its functionalities by implementing Topology Optimization (TO) procedures. Therefore, the developed program is capable of solving different types of topology optimization problems, such as, linear elasticity, thermal conduction analysis and a multi-objective approach. Additionally, it is also possible to perform a linear thermoelasticity analysis, considering a constant temperature field or an updated one coming from a thermal analysis (semi-coupled approach to thermoelasticity). The different approaches can be carried out by the developed software by selecting/deselecting the respective options at the beginning of the process. Therefore, diverse routines associated with each methodology were implemented in order to establish a clean and organized code. In Figure 3.1, it is represented the overall structure of the software GRIDS Alpha with the available procedures specified.

In this section, the structure of the computational tool is presented and some details related to its implementation are specified. Additionally, a summary analysis on each methodology is carried out in order to understand the different options that are available for each procedure.

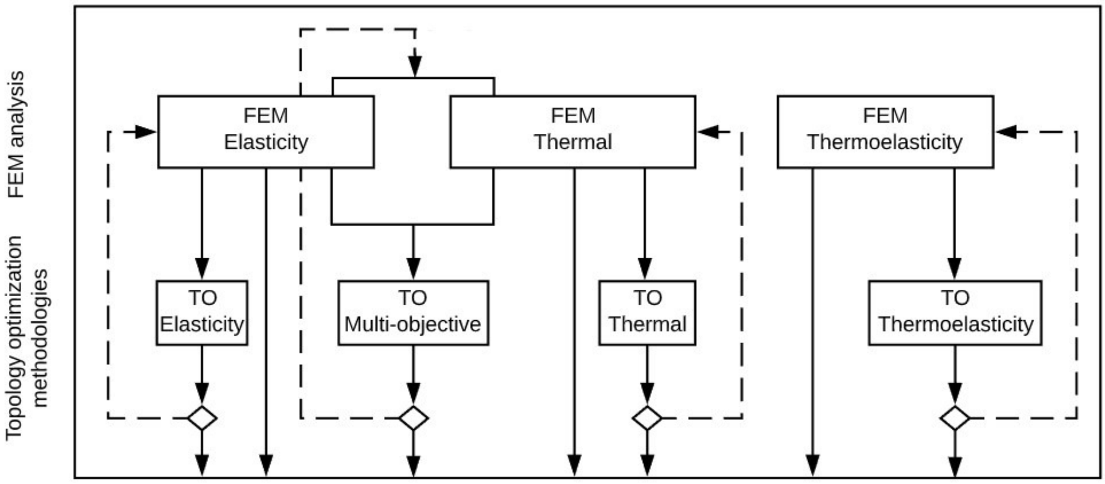

Figure 3.1: Schematic representation of the overall structure of GRIDS Alpha.

3.2 The Finite Element Method

GRIDS Alpha consists in a software that performs numerical analyses of two-dimensional problems. Based on the Finite Element Method (FEM), an elastic analysis can be carried out for different formulations of finite elements. According to the input file introduced by the user, as well as the chosen options, the shape functions and the integration strategy are established for the respective element formulation. The boundary conditions are also initially entered and, on this basis, the stiffness is computed and the equilibrium of the structure established. Consequently, the displacements and the strain and stress levels are determined for the post-processing phase. To perform each phase of the analysis, sub-routines are developed in order to establish an organized code. The implemented sub-routines related to the FEM analysis are used for the thermal and thermoelastic analyses that are developed in this work (*vd.* Sec. 2.1). For the thermoelastic analysis, only a few changes were made with regards to the thermal loads. These have to be computed taking into account the temperature field initially established by the user and, then, assembled to the loads vector. In Figure 3.2, it is illustrated the pseudo-code that shows the incorporation of the thermoelastic analysis in the original software structure.

Define E, v, t, ΔT, $\boldsymbol{\alpha}$
[$\mathbf{f}_\mathrm{m}$]=setNodalForces
if $thermoelastic = 1$ **then**
  Compute thermal loads as Eq. 2.12 — $\mathbf{f}_\mathrm{th}$
  $\mathbf{f} = \mathbf{f}_\mathrm{m} + \mathbf{f}_\mathrm{th}$
else if $thermoelastic = 0$ **then**
  $\mathbf{f} = \mathbf{f}_\mathrm{m}$
end
$\mathbf{U} = \mathbf{K}^{-1}\mathbf{f}$
Compute stress - $\boldsymbol{\sigma}$

Figure 3.2: Pseudo-code for the linear elastic and thermoelastic analyses.

On the other hand, for the thermal analysis, the nature of the problem's variables differ from one another, however, the structure of the problem remains very similar. The applied boundary conditions consist in heat fluxes or prescribed temperatures and the equilibrium equation corresponds to Equation 2.18. Considering that the necessary functions for FEM analysis were already developed, and only specific changes were made, it is not important to detail here all the applied formulation that can be found in [Teixeira-Dias *et al.* 2010].

3.3 Topology Optimization

Since the developed methodologies are based on topologically optimizing a structure submitted to different types of loading, it is crucial to explain, in a general basis, the procedures behind a topology optimization algorithm. A schematic representation of the implemented algorithm is illustrated in Figure 3.3.

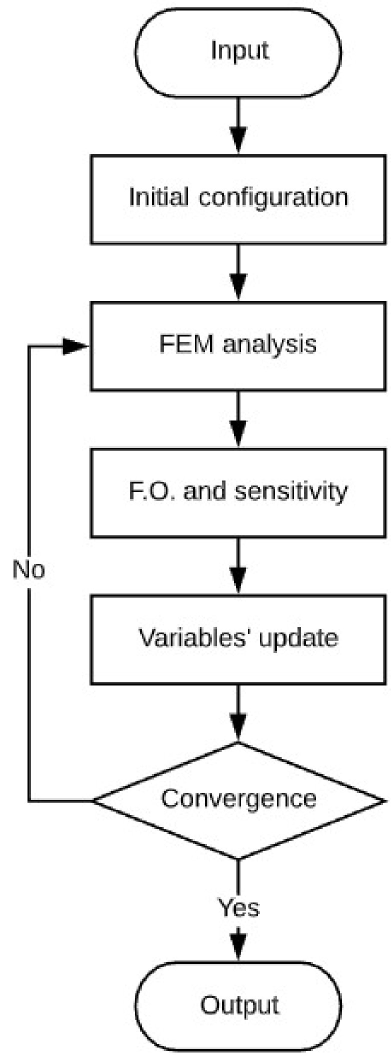

Figure 3.3: Flowchart of the topology optimization algorithm in structural optimization.

For every feature of the software, the process starts by introducing a *.inp* file with the mesh's data. These are analyzed and used to define some important program variables. Initially, the user is prompted to choose the required type of analysis, whether it is a pure-based FEM or a topology optimization. According to the answer, different options are available for each one. The material's properties and the finite element's formulation are established in the developed interface, as well as the prescription of the boundary conditions. Based on the data introduced, the definition of the variables for the optimization process takes place. The initial solution is also established by assigning to each element the volume fraction introduced by the user. All these procedures takes place in the Initial configuration phase.

The next phase consists in the FEM analysis, where the stiffness is computed and assembled as well as the applied loads. Considering a TO problem, it is necessary to take into account the density of the elements for the stiffness' assembly. Thus, in a more efficient way, element stiffness can be computed only at the beginning and, in each iteration, it is only necessary to multiply it by the penalized density of each element. Since the stiffness computation is performed using symbolic variables, it consists in a heavy procedure that can be avoided to be executed in every iteration. Then, the applied loads are correctly assembled and the equilibrium equation is solved in order to establish the structure's equilibrium. As a result from this phase, the displacements of each node are determined taking into account the applied boundary conditions and the material layout. These are necessary to evaluate the objective-function and the sensitivities. This latter evaluation is the most important procedure since it controls the problem's behavior and evolution. Based on their values, each one of the optimization variables is updated by the Optimality Criterion (OC). Alongside the OC method, a bi-sectioning algorithm is carried out to guarantee that the solution respects the volume's restriction. Afterwards, it is applied a convergence criterion to the iterative cycle in order to control the evolution of the problem. In each iteration, a variable (*change*) is determined taking into account the maximum variation of the variables in the respective iteration (*vd.* Fig. 3.4). Based on a limit value defined for the variable *change*, a convergence criterion is established. As long as it is not fulfilled, the optimization process continues until it reaches the optimum solution. However, the topology optimization algorithm is also implemented using a stopping criteria based on the number of iterations (*vd.* Fig. 3.4). The output phase consists in releasing the optimum topology as well as some important variables that are saved for further analysis. Anyway, in each iteration, the obtained topology is presented throughout the process so that the user can follow the evolution.

3.4 Multi-objective approach

A multi-objective approach is also developed in this work by combining the elastic and thermal analyses, developed previously. Therefore, it is possible to evaluate the mechanical and thermal objectives, simultaneously, through a Pareto analysis. In order to control the influence of each one of the objectives in the final solution, it is established a global objective-function as a weighted sum of both functions (*vd.* Eq. 2.26). Since both objectives correspond to quantities of different natures, they can present different values of magnitude. To ensure that the problem is solved based on the weighting defined by the user and not by the magnitude of one of the problems, the normalization of the functions is required. Additionally, it is also necessary to ensure that the optimization algorithms can handle the magnitude of the quantities related to the proposed problems. Therefore, considering the normalized objectives, the implemented methods become independent of the magnitude of the prescribed solicitations, for example. In Figure 3.4, it is represented the pseudo-code related to the evaluation of the global objective-function.

```
change = 1; loop = 0
Initial design - x_new
while change > 0.001 do
    loop = loop + 1
    x = x_new
    ...
    if loop = 1 then
        for i = 1, 2, ..., n do
            c_m^0 = c_m^0 + ρ_i^p u_i^T K_i u_i
            c_t^0 = c_t^0 + ρ_i^p T_i^T K_i T_i
        end
    end
    for i = 1, 2, ..., n do
        c_m = c_m + ρ_i^p u_i^T K_i u_i
        c_t = c_t + ρ_i^p T_i^T K_i T_i
    end
    c = (1 − ω_t) c_m/c_m^0 + ω_t c_t/c_t^0
    ...
    Construct a new design - x_new
    change = max(abs(x_new − x))
    if loop = 100 then
        change = 0
    end
end
```

Figure 3.4: Pseudo-code for the evaluation of the global objective-function in the multi-objective approach.

3.5 Thermoelasticity

Thermoelasticity is the most explored subject in this work because of the challenges it poses regarding topology optimization problems. The study of thermoelastic phenomena involves the evaluation of the derived thermal loads. Therefore, their influence on the optimization process and, consequently, on the optimum topologies is analyzed in detail. That way, three alternative procedures increasingly complex are developed in this work.

In this type of analyses, the computation of the thermal loads represents an important procedure since their value depends on the optimization variables, the elements' relative density. Therefore, their calculation needs to be performed in each iteration taking into account the updated material distribution.

In the first approach (Phase 1), the thermal loads are computed initially for the homogeneous material distribution, considering a structure submitted to a constant temperature field. Over the optimization process, these are kept constant, being only directly considered to the structure's equilibrium. In the following procedure, the thermal loads are already updated in each iteration, taking into account the material distribution. At this point, the sensitivity includes the term related to the design-dependent loads (vd. Eq. 2.41), so it is already possible to analyze their real effect on the obtained solutions. Finally, at the last approach (Phase 3), the temperature field is determined by running a thermal analysis in each iteration, considering the applied boundary conditions (whether they are heat fluxes or prescribed temperatures). Therefore, the thermal analysis is solved and a temperature field is determined. On this basis, the thermal loads are computed in the same way as the previous procedure (Phase 2). Figure 3.5 illustrates schematically the structure of the explained thermoelasticity approaches. The area inside the dashed line represents the loop associated with the topology optimization algorithm. In a similar way to stiffness, the thermal loads are also computed with symbolic values, which consists in a computationally heavy procedure. Since they need to be updated in every iteration due to its dependence on the optimization's variables, their computation is performed initially for the homogeneous material layout and, then, multiplied by the penalized element's density.

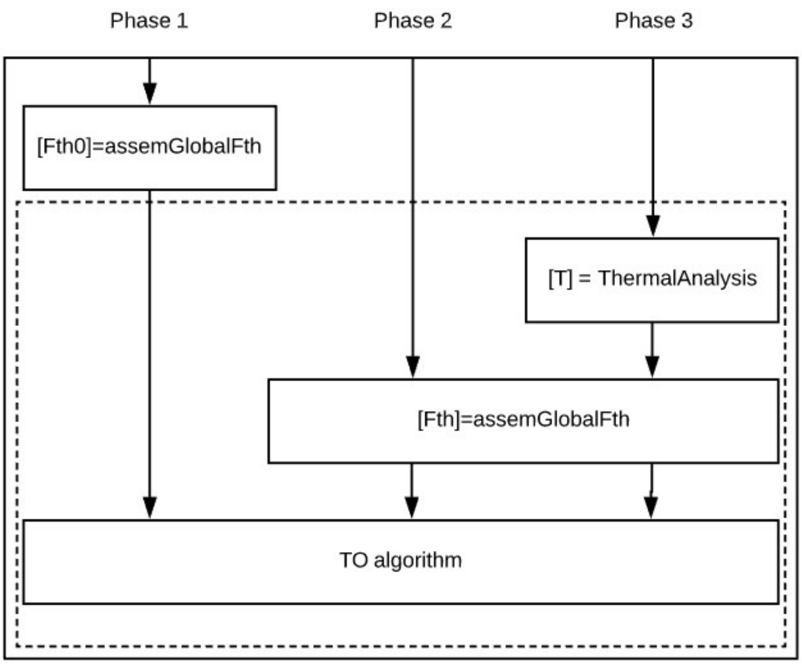

Figure 3.5: Schematic representation of the structure of the thermoelastic procedures.

3.6 Bi-directional Evolutionary Structural Optimization

Several issues appear in thermoelastic problems related to the dependency of thermal loads on the design domain. These issues arise from the existence of terms with opposite signs on the sensitivity, leading to a non-monotonous objective-function. Therefore, in order to overcome these instabilities, an alternative approach to the methodologies explained in section 3.5 is proposed. An extension of the Evolutionary Structural Optimization (ESO) method, known as BESO, is applied to thermoelastic problems considering a constant temperature field. Thus, a sensitivity analysis is also performed in BESO method in order to evaluate the objective-function behavior. The efficiency of each element is analyzed by computing a sensitivity number based on the mentioned sensitivity analysis.

In Figure 3.6, it is represented the pseudo-code for the implemented BESO algorithm. As explained in section 2.3.7, this method presents a different way of solving topology optimization problems when compared to the OC method. In contrast to this, the structure evolves to the optimum topology by decreasing its volume in each iteration. Therefore, the volume of the structure (vol) is initialized as 1 as well as each element's density. The user chooses initially the required volume fraction ($volfrac$) and some parameters such as the penalization factor (p) and the evolutionary ratio (ER). The latter one controls the evolution of the optimization problem by establishing, at the beginning of each iteration, the target volume of the iteration (vol). After the evaluation of the objective-function, the sensitivity number is computed for each element, based on a sensitivity analysis. As explained in section 2.3.8, a filtering scheme is then applied to the sensitivity numbers in order to avoid the appearance of numerical issues on the optimum topologies. The filtered sensitivity numbers are also averaged with those from the previous iteration to ensure the convergence of the problem (*vd.* Eq. 2.54). Afterwards, the update of the variables takes place in a similar way to the OC method. The whole optimization process is controlled by a convergence criterion that is initially established. The convergence parameter (*change*) is computed in each iteration taking into account the evolution of the objective-function in the last iterations. As long as its limit value is not achieved, the process continues until the criterion is fulfilled.

Define BESO parameters: $volfrac$, ER, p, N
$vol = 1$; $change = 1$
Initial solution — $\rho_i = 1$
while *change>0.001* **do**
  $k = k + 1$
  vol=max(vol(1-ER),$volfrac$)
  FEM analysis — $\mathbf{K}$ and $\mathbf{u}$
  Compute the objective-function — $c(\rho)$
  for $i = 1, 2, ..., n$ **do**
    if $\rho_i = 1$ **then**
      $\alpha_i = \frac{1}{2}\mathbf{u}_i^{\mathrm{T}}\mathbf{K}_i{}^0\mathbf{u}_i - \mathbf{u}_i{}^{\mathrm{T}}\mathbf{f}_{\mathrm{th},i}{}^0$
    else if $\rho_i = \rho_{\min}$ **then**
      $\alpha_i = 0$
    end
  end
  Filter the sensitivity numbers as Eq. 2.58 — $\hat{\alpha}_{i,k}$
  $\tilde{\alpha}_i = \frac{1}{2}\left(\hat{\alpha}_{i,k} + \hat{\alpha}_{i,k-1}\right)$
  Construct a new design — $\mathbf{x}_{\mathrm{new}}$
  if *k>10* **then**
    $change = \frac{\left|\sum_{i=1}^{N}(c_{k-i+1} - c_{k-N-i+1})\right|}{\sum_{i=1}^{N} c_{k-i+1}}$
  end
end

Figure 3.6: Pseudo-code for the bi-directional evolutionary structural optimization algorithm. Adapted from [Huang and Xie 2010].

Chapter 4

Results and analyses

In this chapter, several examples are presented and evaluated in order to validate the methodologies implemented in the developed software. This computational tool is capable of solving different problems related to the Finite Element Method (FEM) analysis and Topology Optimization (TO). The examples shown in this section consist in commonly used benchmarks in structural analysis. In order to validate the obtained results, these are analyzed and compared to the ones presented in bibliography.

In a first phase, a linear elastic, a thermoelastic and a steady-state heat conduction analyses are carried out based on FEM. The linear elastic analysis was already implemented in GRIDS Alpha while the other analyses have been developed during this work. Then, the topology optimization methodologies are evaluated, starting by carrying out a linear elastic and thermal conduction analysis. Through the evaluation of the obtained results, the influence of a filtering technique on the optimum topologies is evaluated. Besides, the analyses are performed for different sizes of meshes in order to study the problem of mesh-dependency. Furthermore, by combining both objectives, mechanical and thermal, a multi-objective approach is also performed. Finally, the influence of thermoelastic phenomena is evaluated according to different approaches, including an alternative procedure, an evolutionary algorithm.

The examples shown in this section are carried out assuming a plane stress state and considering a linear elastic isotropic material, which properties are illustrated in Table 4.1. Also, a four-node bi-linear quadrilateral finite element is used in each analysis, which in GRIDS Alpha is defined as Q4.

Table 4.1: Material properties used in the validation of the implemented methodologies.

Material properties		
Elasticity modulus [GPa]	E	210
Poisson coefficient	ν	0.3
Thermal conductivity [$\mathrm{Wm^{-1}K^{-1}}$]	k	50.2
Thermal expansion coefficient [$\mathrm{K^{-1}}$]	α	11×10^{-6}

4.1 FEM validation

A rectangular thin plate of dimensions 0.25×0.5 m^2 with 0.025 m of thickness is represented in Figure 4.1. As illustrated, the plate is submitted to a superficial load (w) equal to 3×10^6 N/m^2 in its right side and kinematically fixed on the opposite side. The analysis was originally performed by [Kattan 2008] and then used by Rúben Lourenço in order to validate the implemented methodology [Lourenço 2018].

Figure 4.1: Representation of a thin rectangular plane subjected to a superficial load. Adapted from [Kattan 2008].

Figure 4.2 represents the horizontal displacements field resulting from a numerical analysis using a mesh of 21×2 elements. Considering the horizontal displacements, these are null on the left hand side, due to the established support conditions. On the opposite side, the displacement is equal to 7.1429×10^{-6} m.

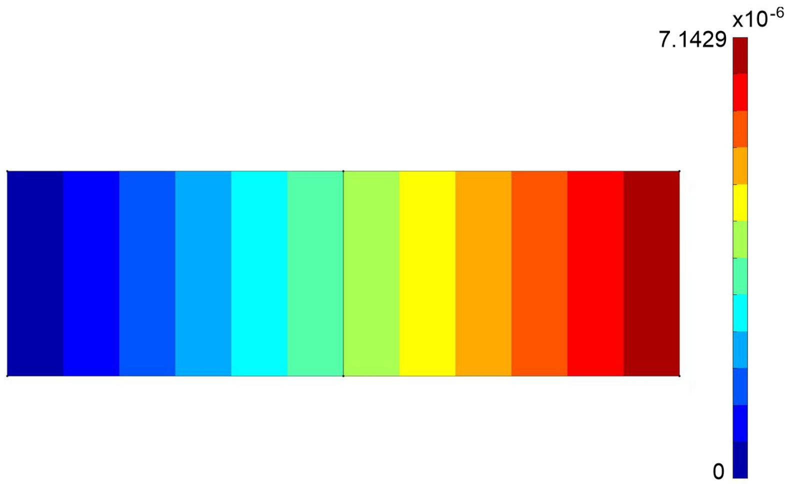

Figure 4.2: Representation of the displacements field for the structure under a superficial loading.

Considering Hooke's Law, the analytical solution to the horizontal displacements in the extremity of the body can be determined by

$$\Delta L = \frac{FL}{EA}, \tag{4.1}$$

where F stands for the total load applied to the center of the extremity, A for the cross-section area, and L for the length of the structure. According to Equation 4.1 and considering F equal to 18750 N, the analytical solution, for $L = 0.5$ m, is 7.1429×10^{-6} m.

The example illustrated in Figure 4.1 is also used to validate the implemented procedure related to the thermoelastic analysis. This analysis and the following ones have been developed in this work taking into account the existing functions for the linear elastic analysis and preserving the modular concept of the software. The structure is under the same predefined loads, but also under a uniform temperature variation, ΔT, equal to 30 K. The displacements due to thermal expansion are no longer negligible and the obtained displacement field is represented in Figure 4.3.

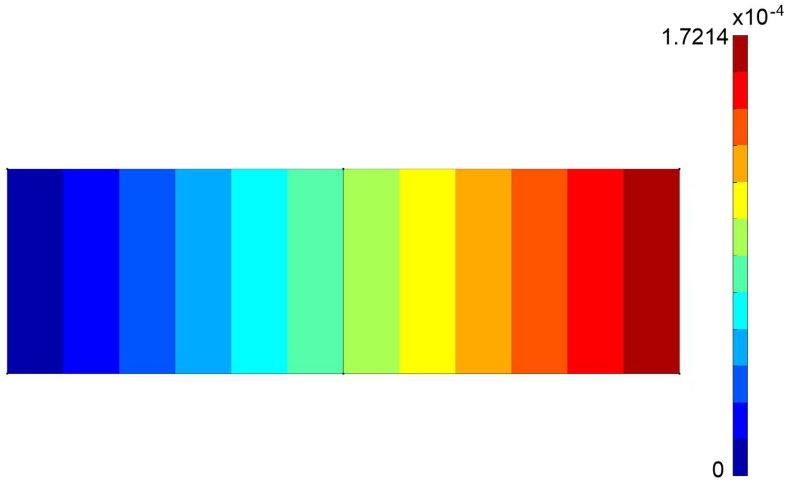

Figure 4.3: Representation of the displacements field for the structure under a superficial loading and a uniform temperature variation.

The illustrated results include the displacements due to mechanical loading and thermal expansion. Considering the displacements related to mechanical loading (*vd.* Eq. 4.1) and subtracting these values to the total ones, the horizontal displacement derived from thermal expansion corresponds to 1.65×10^{-4} m in the free extremity of the structure. This value can be analytically computed by

$$\Delta L = \alpha \Delta T L, \tag{4.2}$$

where L represents the length of structure. ΔT and α stand for the uniform temperature field and the thermal expansion coefficient of an isotropic material, respectively. For $L = 0.5$ m, the extremity of the structure, and $\alpha = 11 \times 10^{-6}$, the analytical solution for the horizontal displacement is equal to 1.65×10^{-4}.

Another example is carried out in order to validate the program considering a structure under bending. Figure 4.4 represents the support conditions and the applied load to a rectangular plate. The plate thickness is equal to 0.001 m and it is considered that the magnitude of the applied load is 100 N. The structure's dimensions are 1×2 m^2. The analysis was carried out for different mesh sizes starting from a mesh of 2×2 elements to 32×32 elements. In order to perform a mesh convergence study, the vertical displacement of the top-right corner node (U2) is analyzed for the mentioned meshes.

Figure 4.4: Representation of a thin rectangular plate under bending.

Therefore, Figure 4.5 represents the convergence of the node's vertical displacement with the increase of the number of elements. In view of the performed analyses, Figure 4.6 illustrates the displacements field using a mesh of 32×32 elements, where the vertical displacement in the right upper corner is equal to 2.2533×10^{-5} m. The obtained results can be compared to the ones presented in the bibliography [Lourenço 2018].

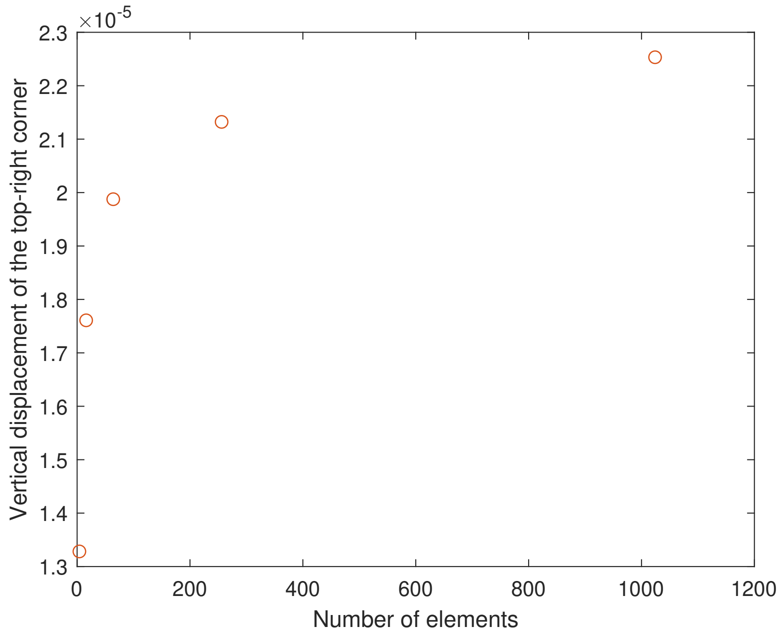

Figure 4.5: Evolution of the vertical displacement of the top-right corner node of the beam.

A thermal analysis is also developed and the illustrated example in Figure 4.7 is used to carry out the mentioned analysis. A two-dimensional square plate of thickness equal to 0.025 m is submitted to a prescribed temperature of 30 °C on its sides and to a uniform heat flux of 5 W/m^2 into the top surface of the plate.

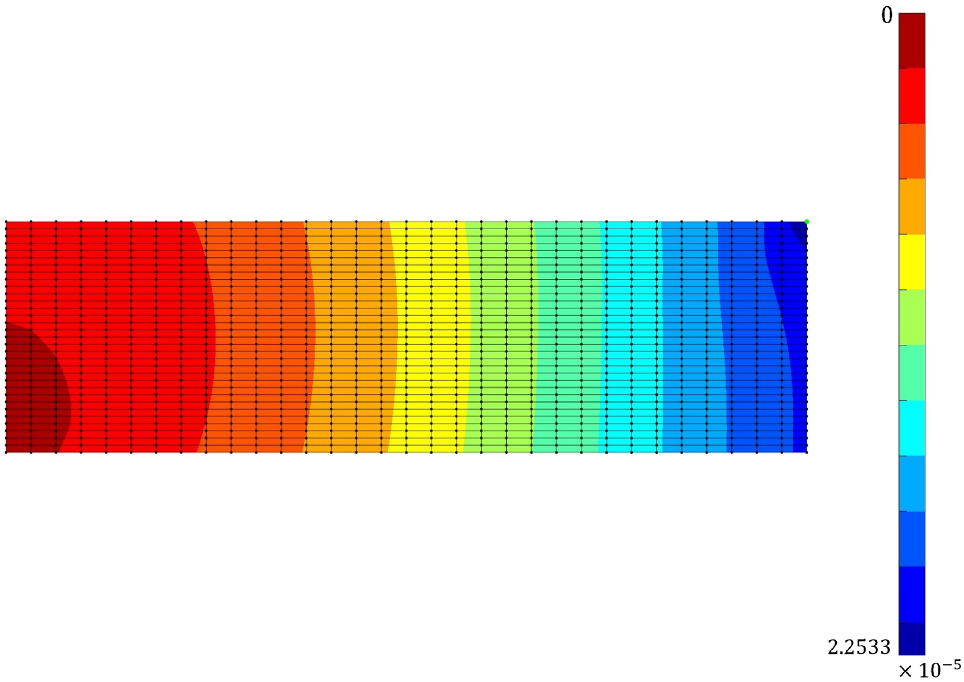

Figure 4.6: Representation of the displacements field for the structure under bending.

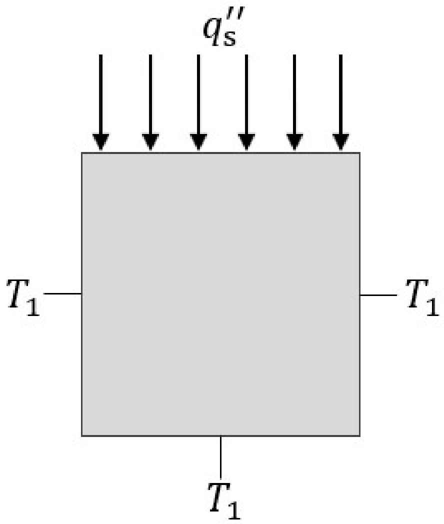

Figure 4.7: Representation of a thin rectangular plate subjected to a heat flux and prescribed temperatures. Adapted from [Incropera *et al.* 2007].

Figure 4.8 represents the temperature field returned by GRIDS alpha using a mesh of 20×20 elements. As expected, the temperature in each lateral node is 30 °C and the maximum temperature is located in the middle node of the top surface and is equal to 103.65 °C.

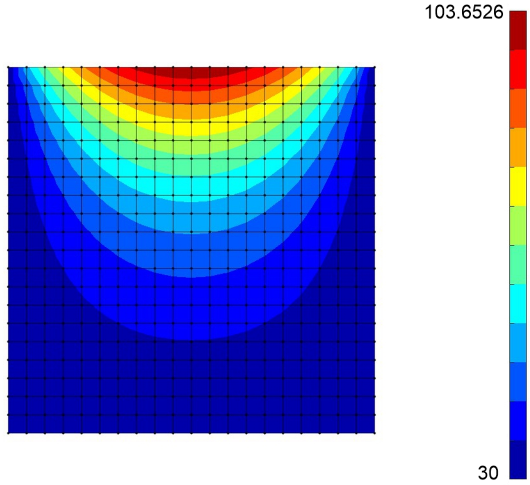

Figure 4.8: Representation of the temperature field of a structure under thermal boundary conditions.

The temperature of each node can be computed by the following equation,

$$q = \frac{kA\Delta T}{L}, \tag{4.3}$$

which represents the Fourier's Law, where k stands for the thermal conductivity coefficient. A and L represent the cross-section area and the length of the plate, respectively. Considering k equal to 110×10^6 W/K^{-1}, the analytical solution for the temperature in the middle of the top surface can be computed. For L equal to 1 m, the dimension of the plate's side, the obtained solution is 103.6526 °C.

4.2 Topology Optimization

Throughout this section, several topology optimization problems are presented and the obtained results are analyzed. Based on 2D examples, the methodologies implemented in this work are validated comparing the obtained results to the ones presented in the bibliography. Initially, a mechanical problem is carried out and the influence of a filtering scheme, as well as of different mesh sizes, is evaluated. Thereafter, a thermal problem is also evaluated and, consequently, a multi-objective approach is considered. Table 4.2 represents the chosen parameters related to the optimization algorithm.

Table 4.2: Optimization parameters used in the resolution of the topology optimization problems.

Optimization parameters		
Penalization factor	p	3
Minimum density	$\rho_{\min}$	0.001
Volume fraction	f_{v}	0.5

A well-known topology optimization problem is illustrated in Figure 4.9. Also recognized as “MBB” beam, the rectangular plate of dimensions 1×3 is represented with a symmetry boundary condition in order to simplify the problem's resolution. Commonly used as a benchmark, this example has already been the focus of several works on topology optimization [Rozvany 1998, Bendsoe and Sigmund 2003, Rozvany 2009].

Figure 4.9: Representation of the “MBB” beam with a symmetry boundary condition. Adapted from [Sigmund 2001].

The proposed problem is solved by using different mesh sizes with 5×15, 10×30, 20×60 and 40×120 four-node bi-linear quadrilateral finite elements. The magnitude of the applied loads is not relevant to the problem's evaluation. Although the sensitivities are dependent on the magnitude of the applied loads and responsible for the optimization process, as long as their variations are consistent, the magnitude of the boundary conditions does not influence the process neither the optimum topologies. Therefore, Figure 4.10 illustrates the obtained results for different sizes of mesh without using any filtering technique. With the intention of validating the optimum topologies, these are compared to the ones from the bibliography [Rozvany 1998, Bendsoe and Sigmund 2003, Rozvany 2009].

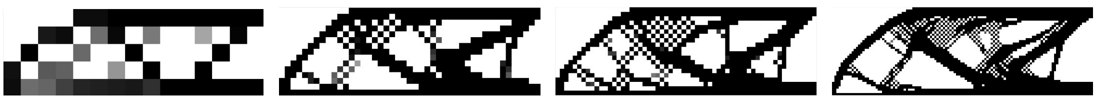

(a) (b) (c) (d)

Figure 4.10: Topologies obtained for different meshes without any filtering scheme.

It is possible to notice the existence of some problems due to numerical instabilities in the results illustrated in Figure 4.10. These issues are described in section 2.3.8 alongside some approaches used to overcome the numerical instabilities. One of the most evident issue is related to checkerboard problems that are caused by the chosen finite element formulation. The existence of checkerboard problems when linear finite elements are used leads to an excessive stiffness of the structure. This suffers from an artificial increase of the stiffness and, consequently, a decrease in the compliance value. Anyway, it is considered a FEM problem and not an optimization one [Rozvany 2009]. On the other hand, this problem can be solved using filtering techniques as also described in section 2.3.8. Although these techniques require an additional computational effort, they allow a more rigorous mesh control and produce topologies without numerical instabilities. A relative radius equal to 1.5 is applied in the filtering scheme keeping the solution's accuracy. As already mentioned, the predefined radius defines the weight of the neighboring elements' density. Based on filtering techniques, the analyses carried out above are repeated using the mentioned filter. The obtained results for these analyses are represented in Figure 4.11.

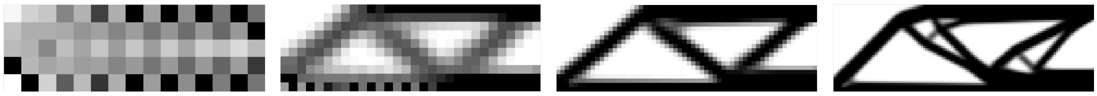

(a) (b) (c) (d)

Figure 4.11: Topologies obtained for different meshes using a filtering scheme.

Checkerboard problems no longer appear in the optimum topologies, leading to the conclusion that the filter produced efficient results. However, intermediate densities start to appear in the optimum topologies between material and void regions. This effect is due to the applied filter that takes into account the density of the elements in the neighbourhood to the new element's density. Besides, the results obtained without using a filtering scheme suffer from mesh-dependency as well as the ones using the filter. As explained in section 2.3.8, the mesh-dependency problem is related to the existence of different optimum solutions for the same problem when using different mesh sizes. This problem could be solved by using a similar filter in order to deal with this issue. Specially, when observing the first topology in Figure 4.11, it is possible to conclude that the mesh in question is too coarse to be possible to apply this filter scheme.

A thermal analysis of a topology optimization problem is carried out in order to validate the developed methodology. Figure 4.12 represents the boundary conditions that are applied to the thermal problem. A heat sink is established in the right bottom node to set the temperature differential to zero in the applied node. In addition, all nodes in the upper and left edges are under a constant heat flux. The same geometry of the "MBB" beam benchmark is used to carry out the thermal analysis for the same mesh sizes used in the mechanical problem. Figure 4.13 represents the obtained results for the thermal analysis using a filtering scheme.

Figure 4.12: Representation of a thermal conduction topology optimization problem. Adapted from [Oliveira 2013].

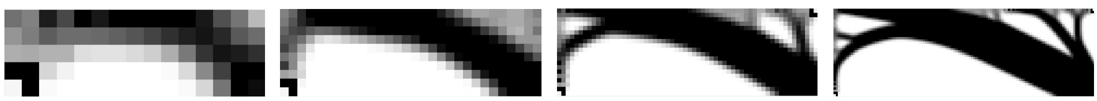

(a) (b) (c) (d)

Figure 4.13: Topologies obtained for different meshes considering a thermal analysis.

The illustrated results were obtained using the filtering scheme shown in section 2.3.8. In a similar way to the results represented in Figure 4.11, it is possible to notice the effect of mesh-dependency in the obtained results. However, the material is allocated considering the pure conduction criteria in order to maximize the thermal conductivity of the structure. The material distribution is established mostly near the heat sink, the right bottom node, and it spreads along the structure toward the edges that are submitted to heat fluxes.

4.2.1 Multi-objective approach

A multi-objective approach is defined by Equation 2.26 which, in this work, considers a structure under mechanical and thermal loading, simultaneously. With the intention of validating the developed program, the problem represented in Figure 4.14 is solved according to the multi-objective approach and its results are analyzed and compared to the bibliography [Oliveira 2013, de Kruijf *et al.* 2007]. A square plate is evenly heated with a constant heat source in all the nodes and in the middle of its left hand side a heat sink is established to set the variation of the temperature's node to zero. On the same side, all the nodes are kinematically fixed and a mechanical load is applied at the middle node of the opposite side.

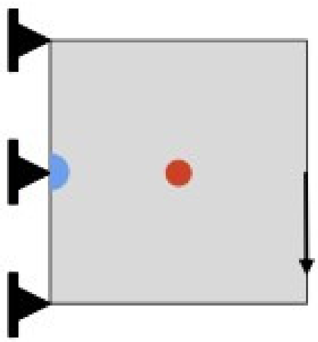

Figure 4.14: Representation of a rectangular plate subjected to a concentrate load and a superficial heat flux. Adapted from [Oliveira 2013].

As explained in Equation 2.26, the global objective-function related to the multi-objective approach is established by normalizing both objective-functions, mechanical and thermal. Moreover, to each objective is assigned a weighting coefficient in order to set its influence on the final solution. Therefore, in Figure 4.15, the optimum topologies for the multi-objective approach are illustrated. The obtained results correspond to values of $w_{\mathrm{t}} = \{0; 0.25; 0.5; 0.75; 1\}$, the weight of thermal analysis. Considering a discretized domain of 80×80 elements and a volume restriction, f_{v}, equal to 0.4, the obtained solutions are similar to the represented in bibliography [Oliveira 2013, de Kruijf *et al.* 2007].

The analysis of the optimum topologies allows the study of the impact of each objective in the optimum solution, according to the predefined weighting coefficient associated with each one. It is possible to notice the evident difference between the optimum solutions of each analysis, namely, the way material is allocated inside the structure for

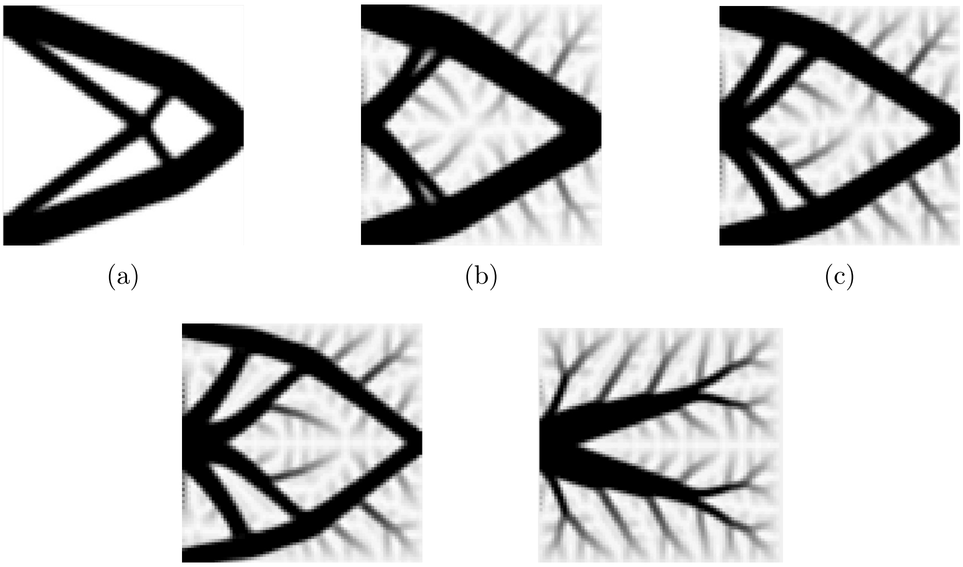

(a) (b) (c) (d) (e)

Figure 4.15: Topologies obtained for different values of w_t considering a multi-objective approach: (a) $w_\mathrm{t} = 0$, (b) $w_\mathrm{t} = 0.25$, (c) $w_\mathrm{t} = 0.5$, (d) $w_\mathrm{t} = 0.75$ and (e) $w_\mathrm{t} = 1$.

each objective independently. On the one hand, the pure conduction criteria establishes the allocation of the majority of material near the heat sink and allows the spread of it along two branches. On the other hand, the majority of the material is allocated over a path between the left and the right upper corners and the application point of the mechanical load, considering the pure elasticity criteria [de Kruijf *et al.* 2007]. The objective-functions of both thermal and mechanical analyses are presented in Figure 4.16a as well as the global objective-function. In Figure 4.16b, the Pareto analysis for this problem is illustrated along with the thermal weighting coefficient, ω_t, of each point.

It is possible to analyze the evolution of the objective-functions over different values of the weight coefficient, ω_t, and also to notice that the optimum points of each objective are not compatible with the other objective in analysis. The evolution of the objective-function to values higher than the initial solution implies an unfeasible solution of the other objective.

4.3 Thermoelasticity

Thermoelasticity comprehends the study of a structure's behavior when subjected to temperature variations due to heat transfer phenomena. Topology optimization of these type of problems brings new issues related to the dependency of the thermal loads on the existence of material. With the purpose of evaluating the influence of thermal loads on topology optimization problems, an example commonly used in the bibliography is carried out and analyzed. Figure 4.17 illustrates a rectangular plate clamped on both sides and subjected to a mechanical load [Rodrigues and Fernandes 1995, Li *et al.* 1999, Gao and Zhang 2010]. In order to evaluate the impact of the temperature on the structure, a thermal expansion coefficient equal to 11×10^{-6} K^{-1} is considered. Moreover, an elasticity modulus equal to 210 GPa is used and a mechanical load of magnitude equal

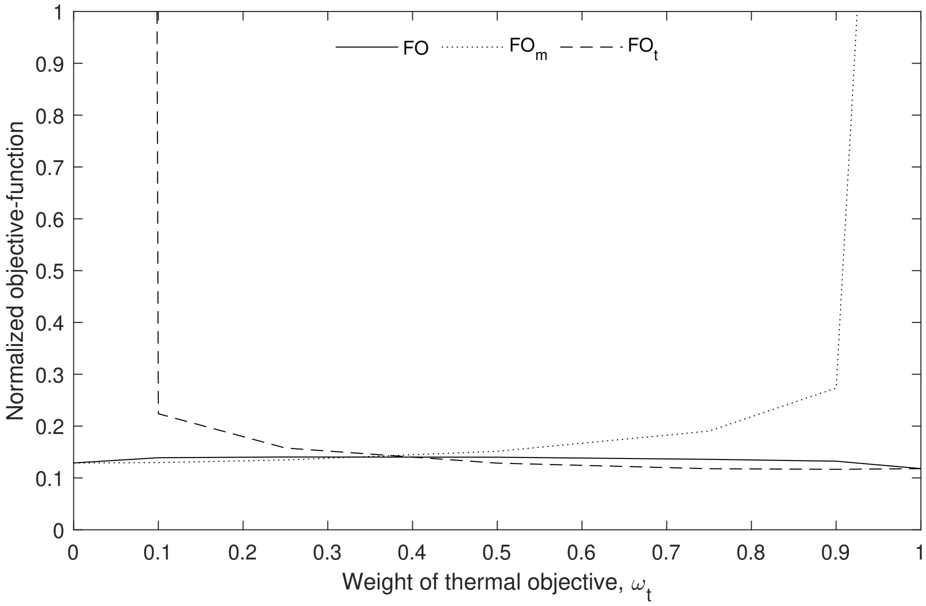

(a)

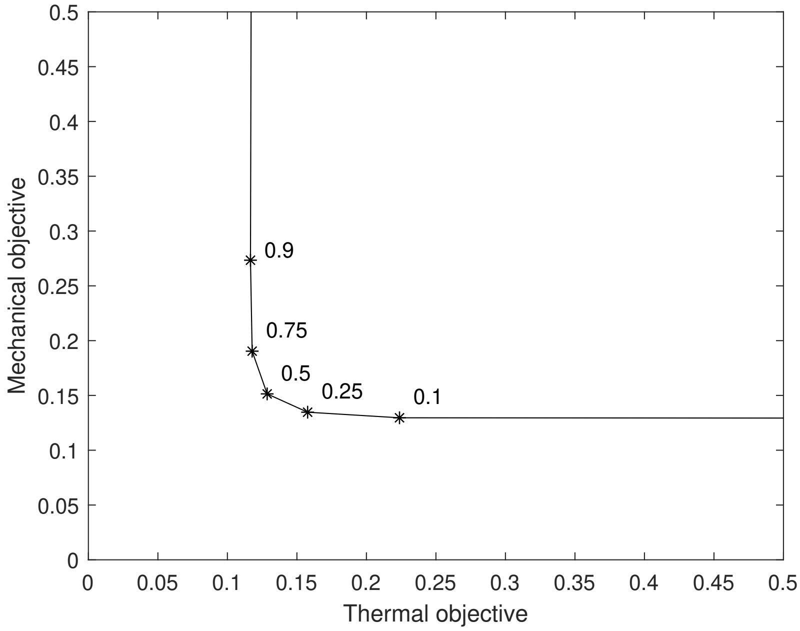

(b)

Figure 4.16: Evolution of a multi-objective topology optimization problem: (a) Mechanical, thermal and global objective-function. (b) Pareto analysis.

to 1×10^5 N is applied to the structure. The same optimization parameters represented in Table 4.2 are used in these analyses.

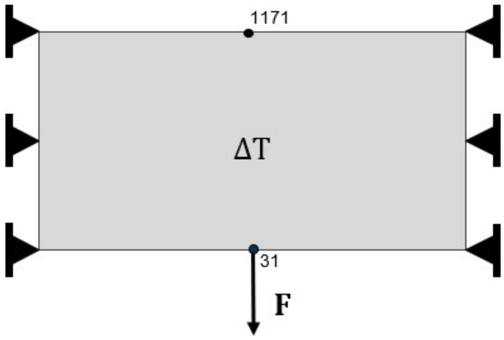

Figure 4.17: Representation of a rectangular plate subjected to a concentrate load and a uniform temperature variation.

The following analyses consist in different approaches that were implemented in order to study and control the influence of thermal loading on the optimum topologies. Firstly, it is considered a uniform temperature variation on the entire structure. The derived thermal loading is initially computed for the homogeneous material distribution and kept constant over the optimization process. Therefore, the impact of thermal loads is not considered in the evaluation of the sensitivities. Several studies are carried out for different values of the temperature differential in order to evaluate its influence on the obtained results, as represented in Figure 4.18.

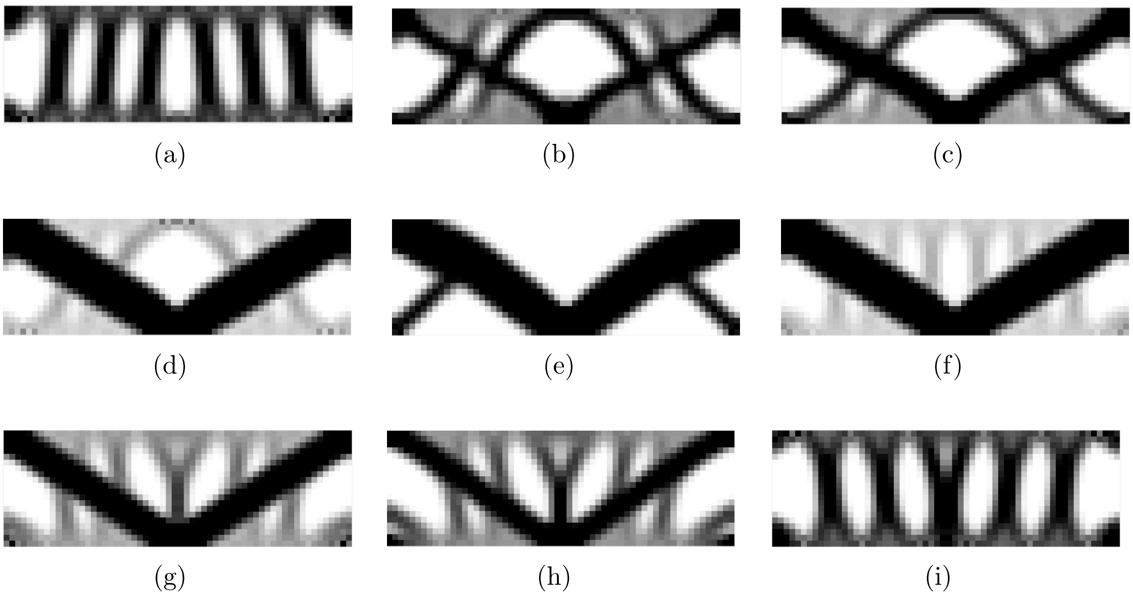

Figure 4.18: Topologies obtained for different values of ΔT considering constant thermal loads over the optimization process: (a) $\Delta T = -10$ K, (b) $\Delta T = -1$ K, (c) $\Delta T = -0.5$ K, (d) $\Delta T = -0.1$ K, (e) $\Delta T = 0$ K, (f) $\Delta T = 0.1$ K, (g) $\Delta T = 0.5$ K, (h) $\Delta T = 1$ K and (i) $\Delta T = 10$ K.

Considering that this phase does not take into account the update of the thermal loading with the material distribution, the obtained results do not reflect the real behavior of a thermoelastic structure. However, even without physical meaning, based on the illustrated topologies, it is possible to notice the material distribution according to the stiffness maximization. Starting with the null temperature differential, the material allocation is mainly established between the middle of the bottom side, the load's point of application, and the upper corners. As the temperature variation increases, the impact of the thermoelastic stress loads starts to be noticed. Although the topology basis remains similar, the material is being allocated differently due to the impact of the thermal loading on the optimization process. In this case, the objective-function sensitivities are still computed taking into account the Equation 2.34. The sensitivity related to the thermal loads is not considered yet, which justifies the reduced instabilities that appear in the optimum results.

The next step consists in the update of the thermal loading in each iteration. Since it depends on the existence of material, its value is updated taking into account the material layout. Besides, the magnitude of the thermal loading is determined based on the quantity of material in each element. The problem illustrated in Figure 4.17 is solved under the same boundary conditions. A mechanical load is applied to the structure with its both sides kinematically fixed and submitted to a uniform temperature variation. Therefore, the obtained topologies are represented in Figure 4.19 for different values of the temperature differential. These results provide important information about the problem's behavior. Along with the objective-function evolution and the local sensitivity on specific elements, it is possible to study the problem's convergence and also to analyze the way thermoelastic phenomena affect the structural behavior. Thus, in Figure 4.20a, it is possible to evaluate the objective-function evolution for different values of the temperature field. Also, the local sensitivities related to elements 31 and 1171, the load's point of application and the superior central element, respectively, are represented in Figure 4.20b.

The obtained topologies correspond to values of temperature variation between -10 K and 10 K. As mentioned, the material converges to the load's application point to maximize the solution's stiffness. However, as the temperature variation increases, it is possible to notice some changes in the material distribution associated with the influence of temperature. Particularly, the impact of the derived thermal loading leads to instabilities on the optimization process. The local sensitivities, in this and the following phases, are computed according to Equation 2.41. It is possible to notice the opposite signals of both terms, which leads to positive and negative values of the sensitivity. This effect is responsible for the non-defined topologies and unstable solutions. The instabilities that appear on the obtained topologies depend on the magnitude of the thermal loads since the impact of a higher temperature differential results in the switch between signs of the sensitivity. This issue affects the objective-function monotony and, consequently, the entire topology optimization process. Until ΔT equal to 0.1 K, the optimum topologies are well defined and reflect the stability of the problem. Besides, it is possible to notice the easy convergence of the objective-function for the same values of ΔT. However, as the temperature differential increases, the objective-function starts to behave in an unstable way, which is more evident when the temperature field reaches 10 K. In this case, for the presented iterations, the problem does not converge to a solution.

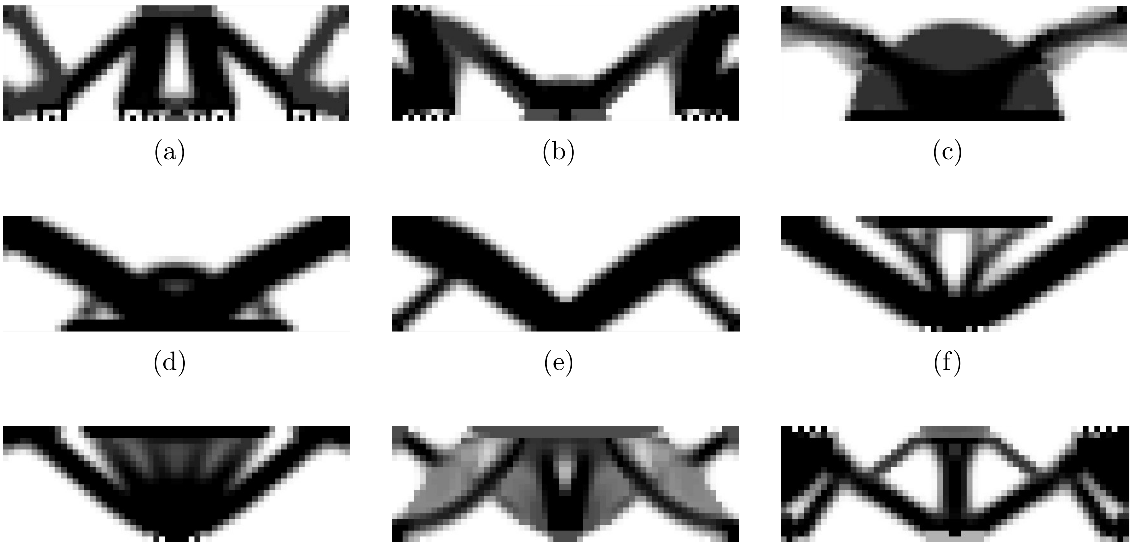

(a) (b) (c) (d) (e) (f) (g) (h) (i)

Figure 4.19: Topologies obtained for different values of ΔT considering a uniform temperature variation: (a) $\Delta T = -10$ K, (b) $\Delta T = -1$ K, (c) $\Delta T = -0.1$ K, (d) $\Delta T = -0.05$ K, (e) $\Delta T = 0$ K, (f) $\Delta T = 0.05$ K, (g) $\Delta T = 0.1$ K, (h) $\Delta T = 1$ K and (i) $\Delta T = 10$ K.

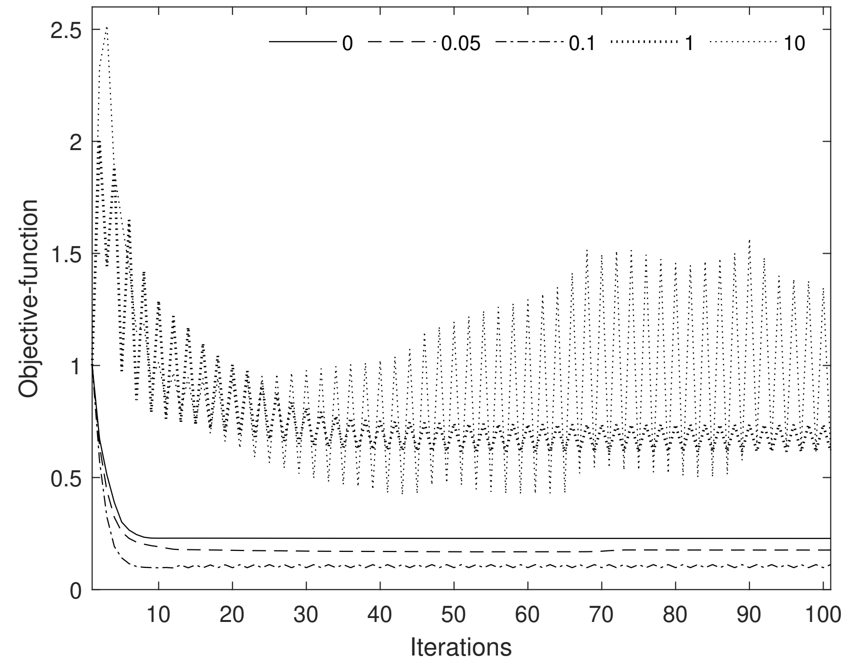

(a)

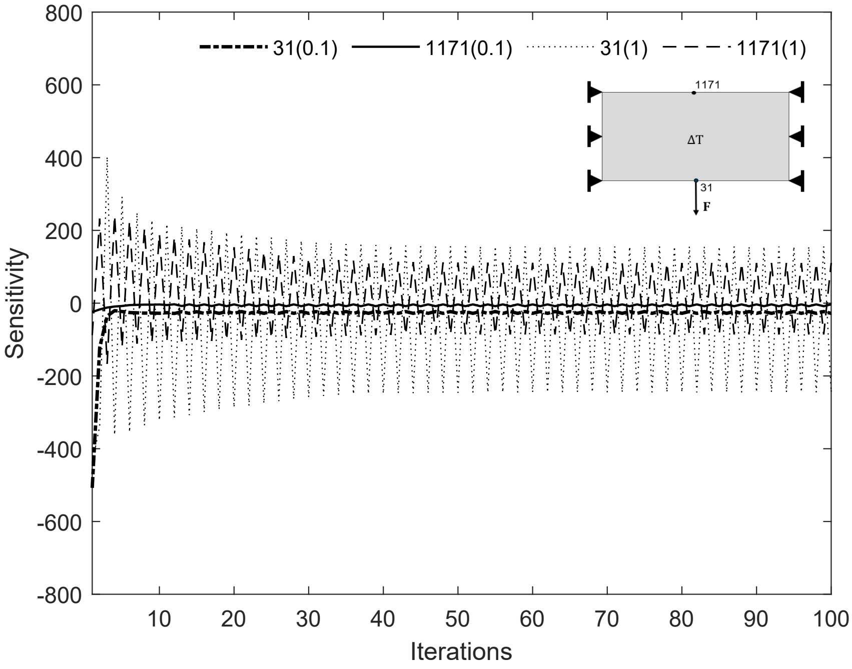

(b)

Figure 4.20: Evolution of a thermoelastic topology optimization problem considering a uniform temperature variation: (a) Evolution of the objective-function. (b) Evolution of the sensitivity on elements 31 and 1171.

Alongside the objective-function, the study of the sensitivity provides information about the evolution of the problem in certain elements. Based on its study, it is possible to compute the impact of thermal loading on each iteration. For instance, in the load's point of application, for $\Delta T = 0.1$ K, the sensitivity is permanently negative since the mechanical problem is still dominant. For the same ΔT, similar behavior is observed on element 1171. Even without the applied mechanical load, the sensitivity remains negative due to the lower impact of the thermal loading. At this range of temperature variation, it is possible to observe a balanced optimization process due to the similar order of magnitude of both loads, thermal and mechanical (1×10^5 N). Otherwise, considering a higher temperature differential, $\Delta T = 1$ K, it is evident the oscillation of the sensitivity value between signs. In this case, the thermal influence overlaps with the mechanical problem, even for the mechanical load's point of application. At this point, it would be expected to have a negative sensitivity since it is where the mechanical problem has its maximum influence. Nevertheless, the influence of the thermal loading is distributed for all the structure and, therefore, it overlaps with the mechanical problem, which is only applied at a single point. Besides, the relation between the magnitude of both loads has changed due to the increase of the temperature differential. The influence of the thermal loading becomes ten times higher than the impact of the mechanical one and, therefore, the problem tends to be more unstable and exposed to the instabilities derived from the impact of the temperature. These instabilities affect the objective-function monotony since the result is always switching between two possible solutions: one of them privileging the stiffness maximization and the other reducing the material quantity to minimize the thermal expansion. Therefore, the problem stabilizes in a divergent one composed mainly by intermediate densities. A valid and stable solution is obtained when the mechanical objective overlaps the thermal one and, therefore, the material would be fully used. Otherwise, when the thermal loading has the major influence in the problem, the only way to minimize the compliance is by eliminating material [Xia and Wang 2008]. This is why Pedersen et al. defend that the minimization of the compliance as the objective-function may be a questionable objective when it comes to thermoelastic problems [Pedersen and Pedersen 2010].

In the last phase, it is proposed to solve the problem illustrated in Figure 4.21. The mechanical boundary conditions are similar to the ones illustrated in Figure 4.17. By contrast, a thermal analysis is carried out to update the temperature field, considering thermal boundary conditions. A heat sink in the middle of the bottom side is set up where the temperature differential is maintained equal to zero along with a heat source applied to the upper side of the plate. Firstly, at the heat source, it is considered the prescription of a temperature differential. In a similar way to the previous phase, the thermal loading is updated in each iteration. However, a varying temperature field is considered taking into account the material distribution and the established boundary conditions.

Initially, the structure is submitted to a varying temperature field due to the prescribed temperature variation on the nodes located in the heat source. The optimum topologies for these analyses are represented in Figure 4.22, for different values of the prescribed temperature differential, ΔT. In Figure 4.23a, the evolution of the objective-function is illustrated alongside the evolution of the local sensitivity on elements 31 and 1171, in Figure 4.23b.

Similarly to the last phase, it is possible to notice the higher stability of the problem

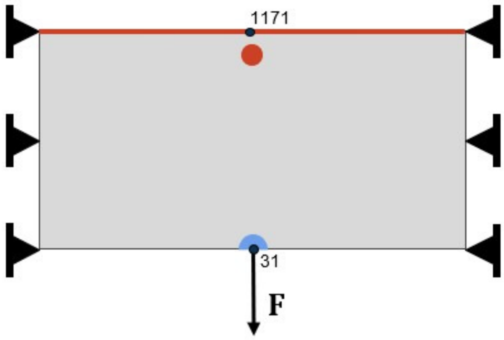

Figure 4.21: Representation of a rectangular plate subjected to a concentrate load and a varying temperature field.

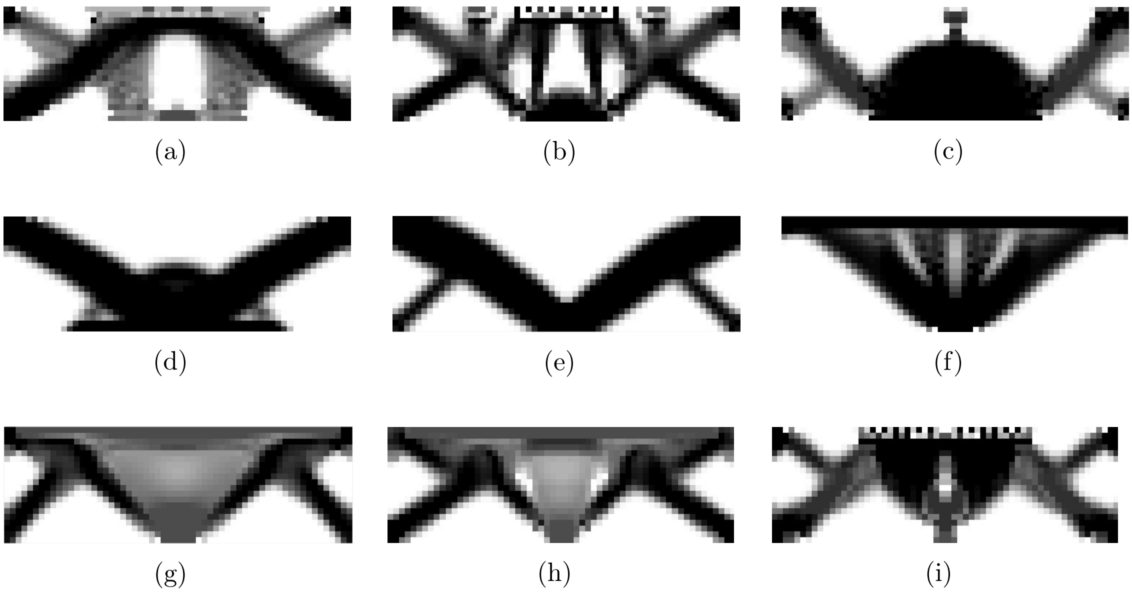

Figure 4.22: Topologies obtained for different values of ΔT considering a varying temperature field: (a) $\Delta T = -10$ K, (b) $\Delta T = -1$ K, (c) $\Delta T = -0.5$ K, (d) $\Delta T = -0.1$ K, (e) $\Delta T = 0$ K, (f) $\Delta T = 0.1$ K, (g) $\Delta T = 0.5$ K, (h) $\Delta T = 1$ K and (i) $\Delta T = 10$ K.

for lower values of the temperature field. Also, for these values, the problem converges to the optimum solution. On the other hand, for higher values of ΔT, the problem is highly unstable and tends to diverge. Considering $\Delta T = 0.1$ K, the sensitivity on both elements is permanently negative since the influence of thermal loading is being overlapped by the mechanical loading. By contrast, for $\Delta T = 1$ K, the sensitivity on both elements is alternately varying between two values, one positive and one negative. The problem can not converge to a solution so it keeps switching between two possible solutions, one prioritizing the stiffness and the other the material expansion. Since in element 31, the influence of the mechanical problem is higher, the sensitivity reaches lower values. On the other hand, in element 1171, the sensitivity varies between a less

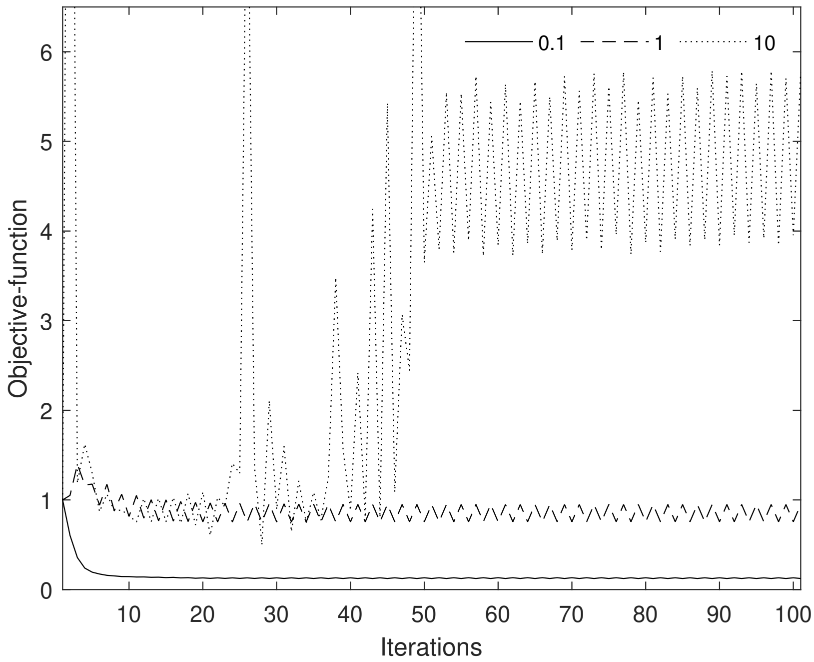

(a)

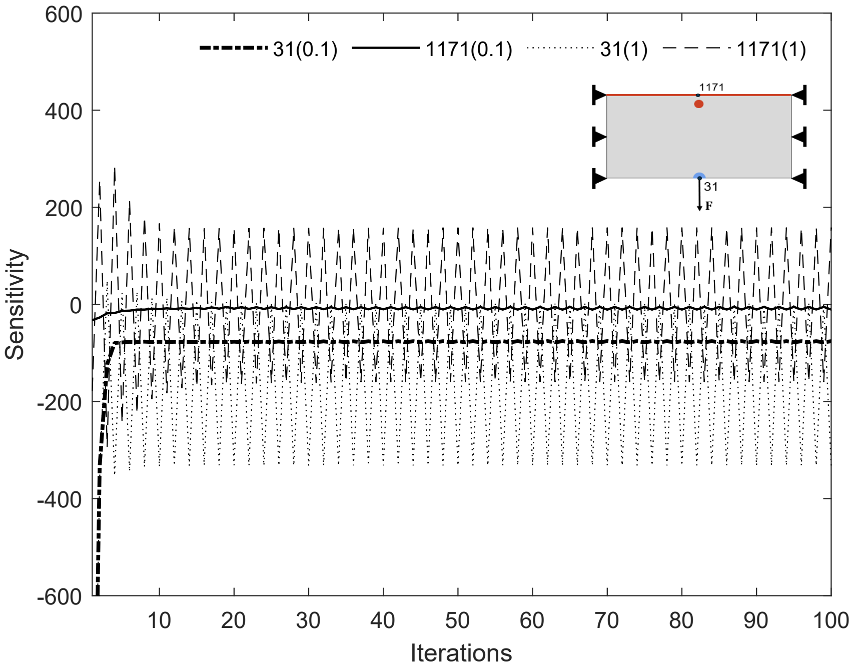

(b)

Figure 4.23: Evolution of a thermoelastic topology optimization problem considering a prescribed temperature variation in the heat source: (a) Evolution of the objective-function. (b) Evolution of the sensitivity on elements 31 and 1171.

negative value and a positive one due to the higher magnitude of the thermal loading. Furthermore, considering higher values of ΔT, it is noticeable the increase in the number of elements with intermediate densities in the optimum topologies and, also, the appearance of checkerboard problems related to the influence of the thermal loading.

Finally, a prescribed heat flux is established on each node of the heat source instead of the prescribed temperature differential. Different values of the nodal heat flux, q, are evaluated and the obtained results are illustrated in Figure 4.24. It is possible to evaluate the high instability associated with the objective-function in Figure 4.25.

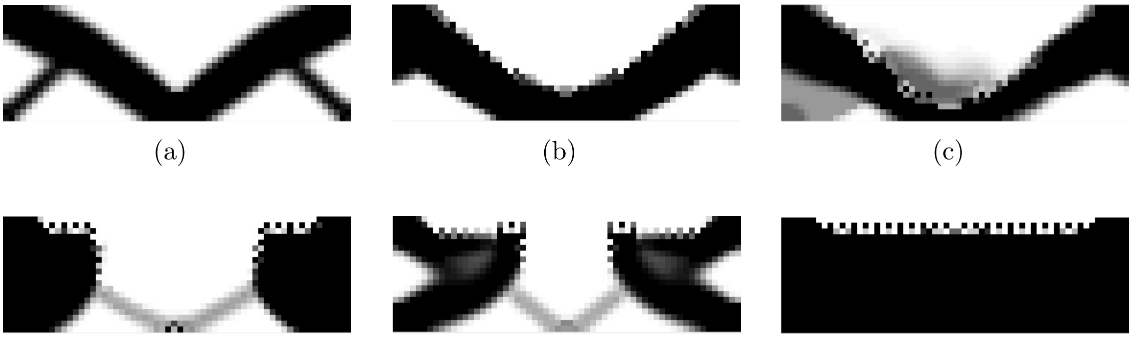

(a) (b) (c)

(d) (e) (f)

Figure 4.24: Topologies obtained for different values of q considering a varying temperature field: (a) $q = 0$, (b) $q = 1 \times 10^{-10}$, (c) $q = 1 \times 10^{-9}$, (d) $q = 5 \times 10^{-9}$, (e) $q = 1 \times 10^{-8}$ and (f) $q = 1 \times 10^{-7}$.

Both problems rely on a thermal analysis to obtain the respective updated temperature field. The applied boundary conditions, as well as the problems' nature, are very similar. However, the obtained results differ in some aspects. The prescription of a temperature differential leads to a gradual reduction of the temperature variation between the heat source and the heat sink. Therefore, the impact of the thermal loading, *i.e* the material expansion, is consequently reduced. Thus, the optimum solutions are more defined topologically. On the other hand, the prescription of heat fluxes, even for low values, leads to the divergence of the problem. These analyses consider the heat fluxes as predefined energy fluxes, which are responsible for the high instability of the results. In the absence of the necessary quantity of material to conduct the heat, the thermal gradients get bigger. Consequently, the thermal loading increases along with the derived thermal expansion. To reverse this effect, the density is reduced once again leading to a cycle of instabilities and, consequently, to the instantaneous divergence of the problem [Oliveira 2013]. This effect can be seen in Figure 4.24f, where the impact of the thermal loading becomes evident. In this case, the obtained solution does not consist in a feasible and possible one, since the volume restriction has not been fulfilled. Due to the high impact of the derived thermal loading, the structure can not dissipate all the heat only with the volume fraction that has been prescribed. So, a larger quantity of material is used in order to provide the necessary heat dissipation and the structure's equilibrium. Additionally, the same numerical effects can be shown in both cases, being the topologies characterized by the existence of checkerboard problems for higher values of the temperature differential on the structure.

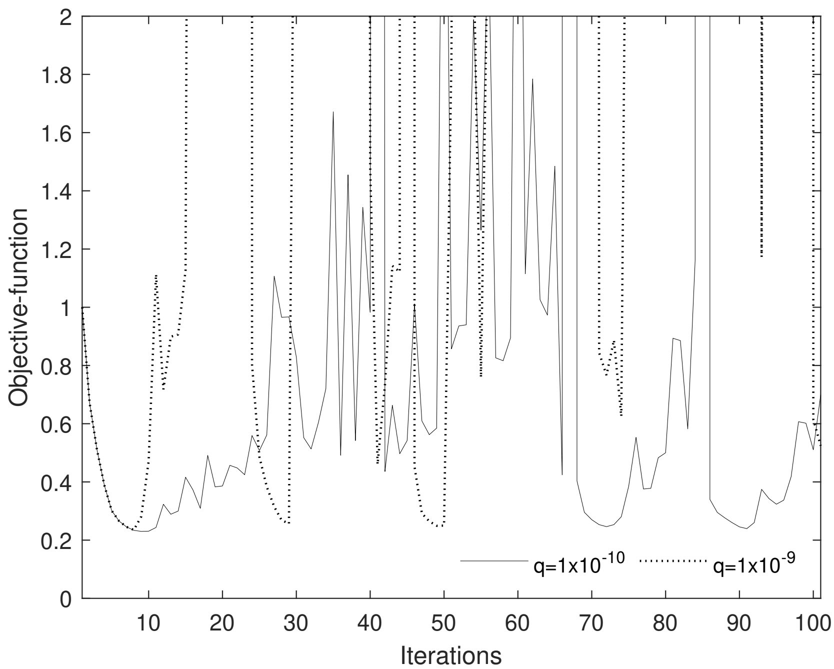

Figure 4.25: Evolution of the objective-function for a thermoelastic topology optimization problem considering prescribed heat fluxes in the heat source.

4.4 Bi-directional Evolutionary Structural Optimization

Several issues have been pointed out concerning problems where boundary conditions depend on the solution. This work analyzes thermoelastic phenomena in the context of a topology optimization problem, namely, the existence of loads that depend on the variables of optimization, *e.g.* thermoelastic stress loads. These loads raise several questions that are presented and discussed in the analyses carried out in section 4.3. As explained in section 2.3.5, these issues result from the existence of two terms with opposite signs in the sensitivity of the objective-function (*vd.* Eq. 2.41). Depending on the magnitude of the thermal loads, the sensitivity can assume positive and negative values. Therefore, the constant switch between positive and negative values leads to instabilities on the optimization process and on the optimum topologies. With the intention of solving the mentioned issues and stabilizing the optimization process, this work proposes the implementation of an alternative approach. An adaptation of the Evolutionary Structural Optimization (ESO) algorithm is evaluated to try out its effectiveness to solve the issues mentioned before. Known as Bi-directional ESO (BESO), this method introduces a different way of topologically optimizing a structure. The OC method assumes from the beginning that the structure's volume is equal to the prescribed volume fraction, and from then on, several possible solutions show up until the optimum solution is reached. By contrast, the BESO method assigns to the initial solution the total possible volume, *i.e*, the volume fraction equal to 1. Therefore, the structure evolves toward an optimum material distribution with its volume decreasing over the optimization process until it reaches the required volume fraction. Thus, the same example carried out in section 4.3

considering a structure submitted to a uniform temperature variation is evaluated by the BESO method (*vd.* Fig. 4.17).

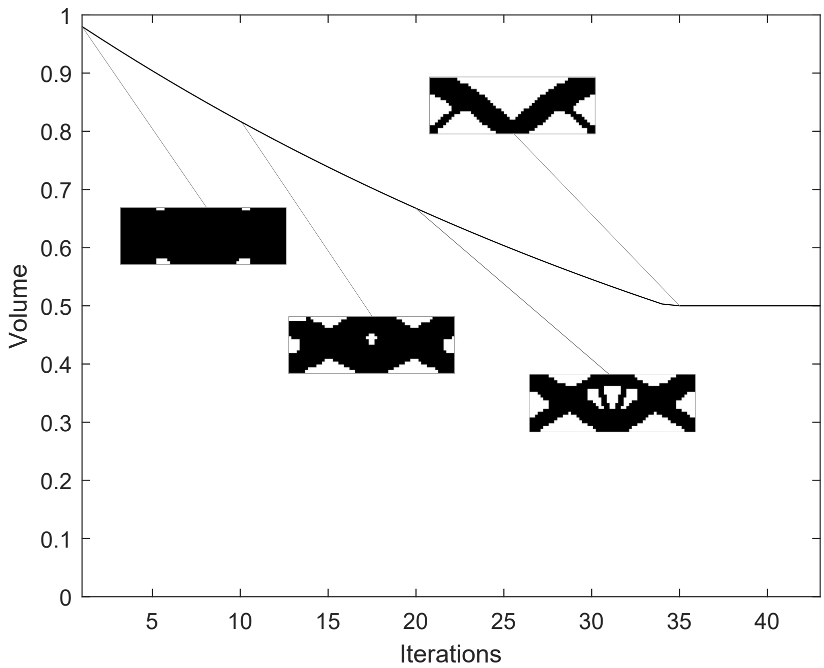

Figure 4.26: Evolution of the volume of the structure using BESO method.

In Figure 4.26, it is represented the evolution of a structure's volume over the optimization process considering the temperature differential equal to 0, according to a "hard-kill" approach. In a similar way to the ESO method, it is assigned initially the total volume to the structure ($f_\mathrm{v} = 1$) and, then, at each iteration, the less efficient elements are removed based on their sensitivity numbers. However, the BESO method also allows elements to be added in the locations next to those elements with highest sensitivity numbers apart from removing those in regions with lowest sensitivity numbers [Huang and Xie 2010]. Over the optimization process, the structure's volume decreases since the number of elements that are removed is higher than the number that are added. Once the target volume is reached (iteration 35), the number of elements that are added is equal to those which are removed. However, the obtained topologies resulted from the following iterations also consist in possible solutions to the problem, leading to a failed achievement of a convergence optimal solution. As a result, the best solution has to be chosen by comparing a large number of solutions generated during the optimization process [Rozvany 2009]. Anyway, the same evolution can be noticed when considering a structure submitted to a uniform temperature variation. Therefore, the example illustrated in Figure 4.17 is evaluated considering the same boundary conditions. Figure 4.27 illustrates the obtained results for different values of the temperature differential.

The presented topologies allow, in a first analysis, to determine the similarity between the obtained results and the conventional method (*vd.* Fig. 4.19). The global topology is similar, mostly, for lower values of the temperature differential. Furthermore, it is possible to notice the non-existence of intermediate densities, which represent a disadvantage of the conventional material interpolation scheme SIMP. In contrast, the evolu-

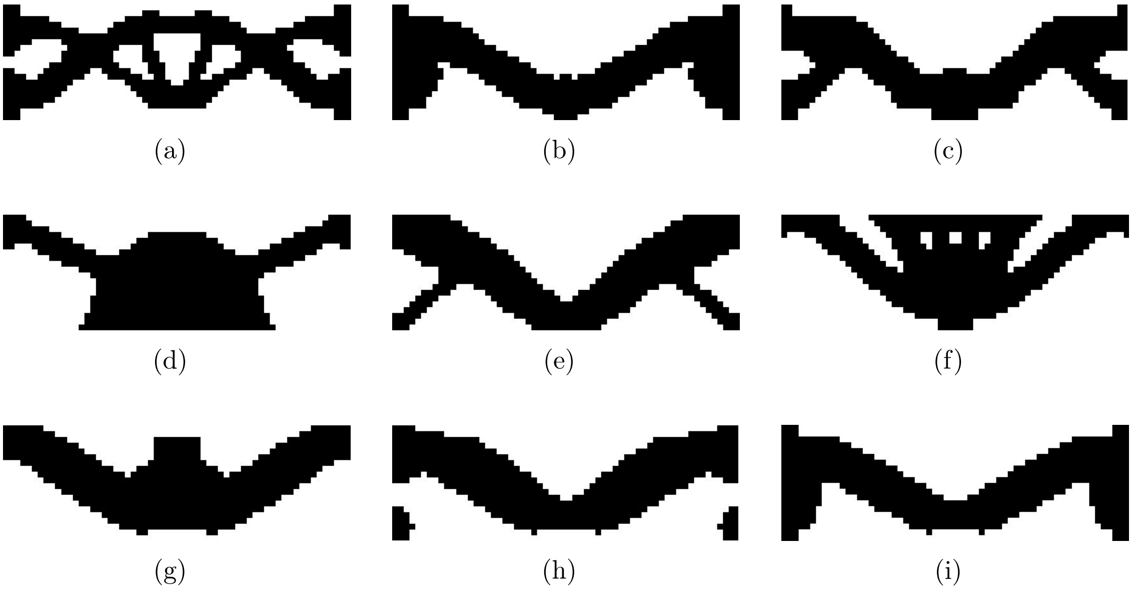

Figure 4.27: Topologies produced considering a “hard-kill” approach and $ER = 0.02$ for different values of ΔT: (a) $\Delta T = -10$ K, (b) $\Delta T = -1$ K, (c) $\Delta T = -0.5$ K, (d) $\Delta T = -0.1$ K, (e) $\Delta T = 0$ K, (f) $\Delta T = 0.1$ K, (g) $\Delta T = 0.5$ K, (h) $\Delta T = 1$ K and (i) $\Delta T = 10$ K.

tionary structural optimization method establishes the use of discrete variables, so the optimum topologies are more defined when compared to those resulting from SIMP, being considered an advantage of the ESO method. With regard to the objective-functions' evolution, in contrast to section 4.3, the analyses carried out related to BESO do not present normalized objective-functions due to the unstable behavior associated with their optimization processes. Therefore, the evolution of the objective-functions correspondent to the null temperature differential and equal to 0.1 is illustrated in Figure 4.28. It is possible to observe the instability associated with the $\Delta T = 0.1$, which remains similar for higher values of ΔT even when the obtained topologies are well defined. The high values of the objective-function are related to a considerable deformation of some elements of the structure and not necessarily to the problem's instability. Moreover, as it can be noticed, considering the temperature differential null, the objective-function is not decreasing, by contrast, it is increasing. As you go through the optimization process, the volume becomes increasingly small which leads to a structure more and more fragile. That way, in each iteration, the structure's compliance becomes higher. Once the volume reaches the target value (iteration 35), the objective-function stabilizes in a constant value, which means that the convergence has been achieved. However, for $\Delta T = 0.1$, the convergence is not achieved due to the problem's instability. Therefore, from iteration 35, several possible solutions are presented until the problems diverges in iteration 56. Figure 4.29 illustrates the evolution of the sensitivity number on element 31, the load's point of application, for $\Delta T = 0$, $\Delta T = 0.1$ and $\Delta T = 1$. Considering the structure under only mechanical loading, it is possible to notice the stability of the sensitivity number. Its value is almost always constant and the magnitude is related to the influence of the mechanical loading, the positive term of the sensitivity number. With the increase of the temperature differential, the sensitivity number tends to behave in a more unstable way. The impact of the thermal loads increases and the sensitivity number decreases as a consequence of the negative sign of the term related to the thermal loads of the sensitivity. Considering $\Delta T = 1$, it is possible to observe the switch of the sensitivity number between two solutions. The same behavior was noticed in the results from the conventional method (*vd.* Fig. 4.20). Although the sensitivity is used in a different way in both methods, both are known as gradient-based methods. So, the same behavior is observed and it is caused by the opposite signals of both terms in the sensitivity number. Thereby, in a similar way to the sensitivity number, the density of the element is always switching between 1 and ρ_{min} with the change of the sensitivity number in the respective element.

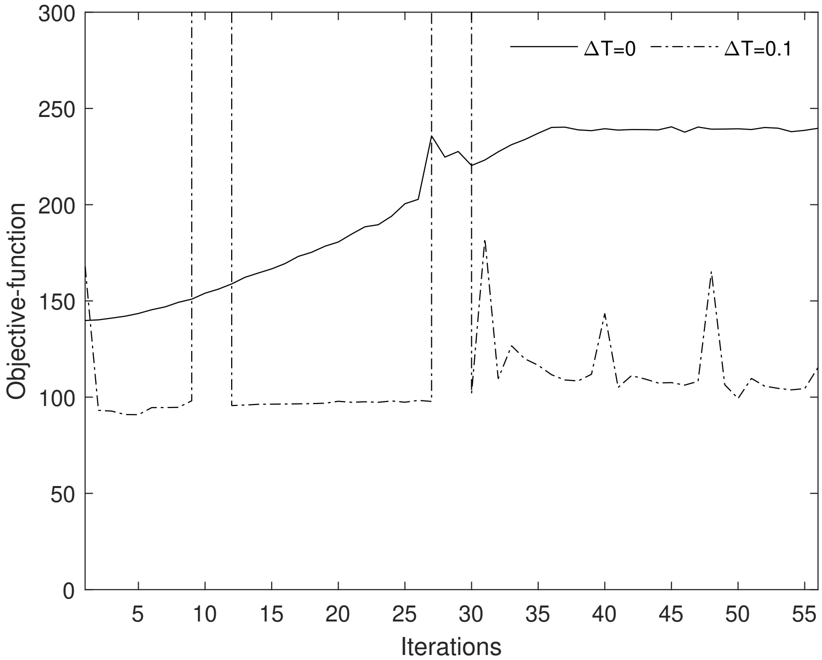

Figure 4.28: Evolution of the objective-function considering a "hard-kill" approach and $ER = 0.02$.

The BESO method defines some parameters that are very important to the optimization process as well as to its convergence. The evolutionary ratio (ER) is one of them. This parameter is initially established by the user and its value defines the progress of the optimization process. At the beginning of each iteration, the target volume for that iteration is determined based on the volume fraction and, mainly, on the evolutionary ratio. Therefore, according to its value, the amount of elements that are going to be added or removed is defined. Consequently, a higher value establishes a faster process until the target volume, namely, the prescribed volume, is achieved. However, the problem tends to diverge more easily since the structure is submitted to large changes in each iteration. On the other hand, a lower value establishes a slower process, but more restrained. Therefore, in contrast to Figure 4.27, where the topologies were obtained using $ER =$ 0.02, Figure 4.30 illustrates the obtained topologies for different values of

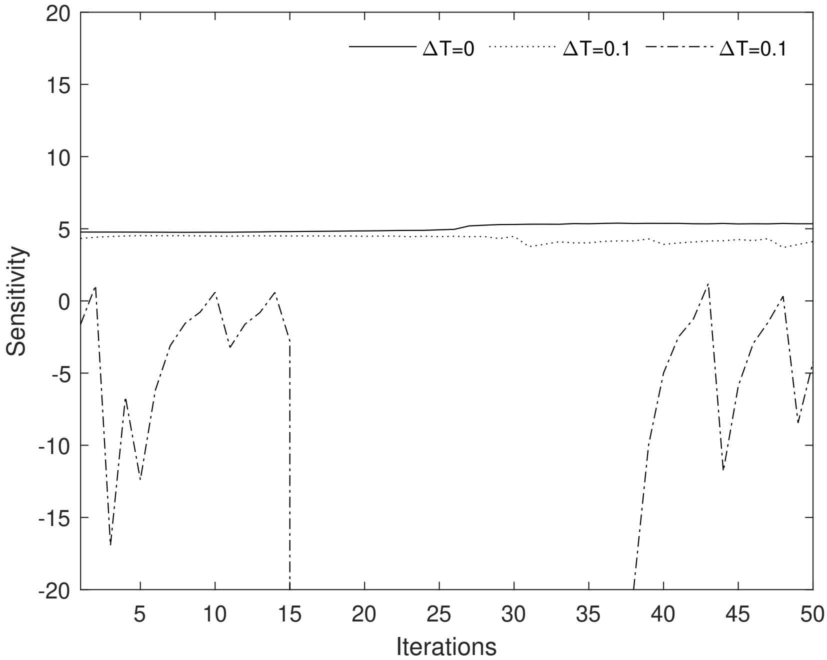

Figure 4.29: Evolution of the sensitivity on element 31 considering a "hard-kill" approach and $ER = 0.02$.

ΔT, considering an evolutionary ratio equal to 0.01.

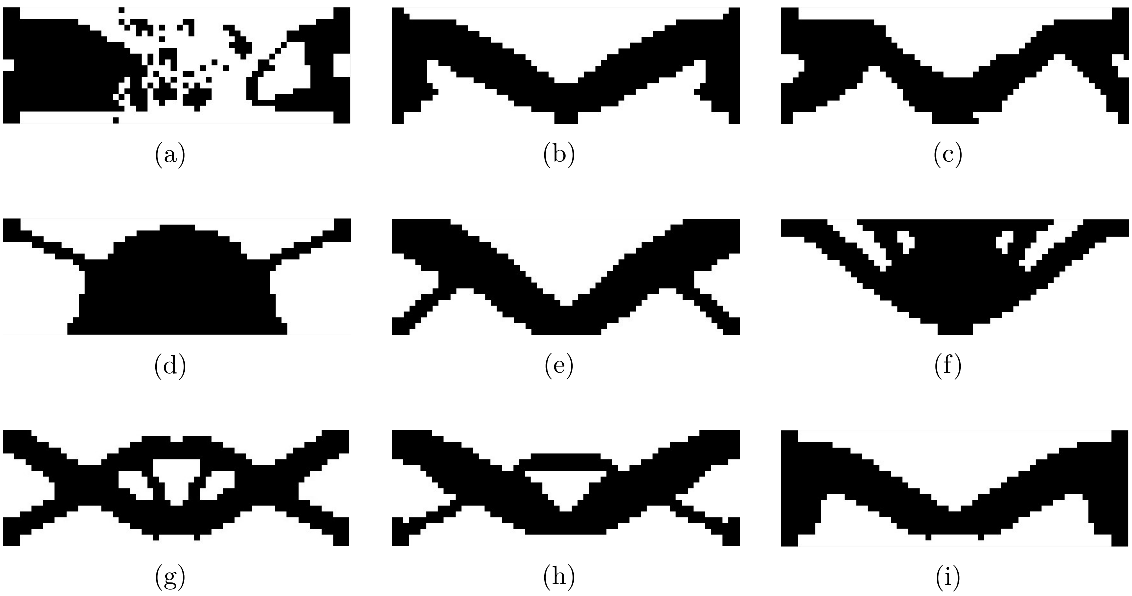

Figure 4.30: Topologies produced considering a "hard-kill" approach and $ER = 0.01$ for different values of ΔT: (a) $\Delta T = -10$ K, (b) $\Delta T = -1$ K, (c) $\Delta T = -0.5$ K, (d) $\Delta T = -0.1$ K, (e) $\Delta T = 0$ K, (f) $\Delta T = 0.1$ K, (g) $\Delta T = 0.5$ K, (h) $\Delta T = 1$ K and (i) $\Delta T = 10$ K.

The obtained topologies are quite similar to those illustrated in Figure 4.27, specially for lower values of the temperature differential. For example, considering $\Delta T = -10$, the optimization process diverges before reaching the target volume, even considering a lower value of the evolutionary ratio. In contrast, the optimum topology, when a higher value of ER is taken into account ($ER = 0.02$), consists in a possible solution to the problem and a well defined material layout (*vd.* Fig. 4.27a).

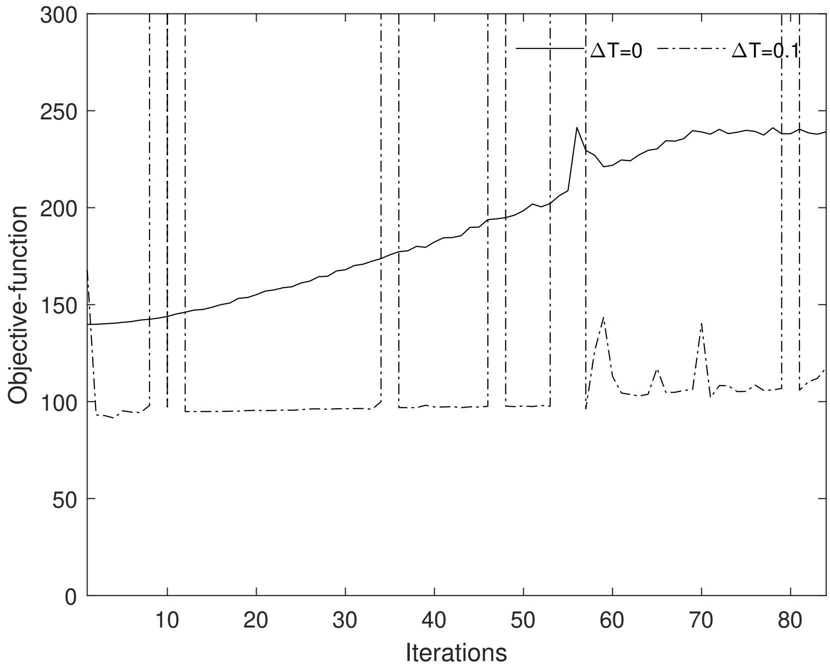

Figure 4.31: Evolution of the objective-function considering a “hard-kill” approach and $ER = 0.01$.

Figure 4.31 represents the evolution of the objective-functions for values of the temperature differential equal to 0 K and 0.1 K, considering $ER = 0.01$. Compared to Figure 4.28, the evolution of both objective-functions are quite similar. However, considering $\Delta T = 0.1$, an evolutionary ratio equal to 0.02 leads to a more stable objective-function. On the other hand, the final values of the objective-functions for both cases are rather similar. In addition, as mentioned before, the convergence of the optimization process is faster when a higher value of ER is considered. The opposite happens when a lower value ($ER = 0.01$) is established leading to a slower process. Therefore, the convergence is achieved later. In addition, it is possible to evaluate the evolution of the sensitivity number on element 31 for both values of ER, 0.01 and 0.02, in Figure 4.32. Moreover, it is noticeable that the parameter $ER = 0.02$ leads to a faster optimization process, being the target volume achieved at iteration 35. However, near the iteration 30, the process starts to diverge due to the large changes that the structure is submitted to. By contrast, considering $ER = 0.01$, the problem only reaches the volume fraction at iteration 69, since the volume of the structure is slowly decreasing when compared to the opposite approach. At this point, the problem tends to behave in a more unstable manner, however, during the optimization process, the sensitivity had remained almost

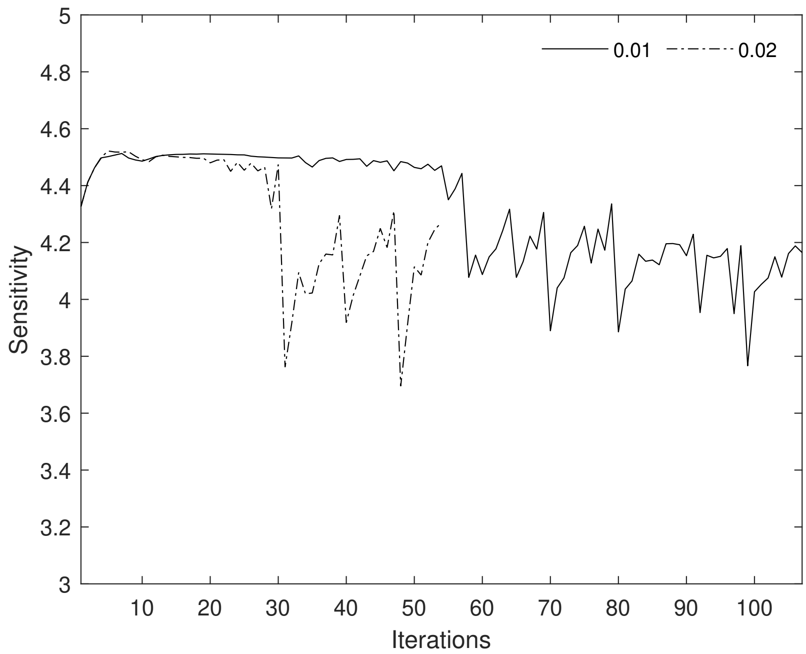

Figure 4.32: Evolution of the sensitivity on element 31 for both values of ER considering a "hard-kill" approach and a uniform temperature variation equal to 0.1.

constant.

The results presented and evaluated previously correspond to the "hard-kill" approach. As mentioned in section 2.3.7, this approach consists in a specific case of the "soft-kill" one when the penalization factor tends to infinity. Both procedures are similar with the exception of the computation of the sensitivity number for void elements. According to the "hard-kill" method, the sensitivity number is equal to zero for void elements. By contrast, the "soft-kill", based on the SIMP method, defines a sensitivity number that depends on the penalization factor and on the minimum density established for void elements. Therefore, the optimization process behaves in a different manner leading to different optimum solutions. Figure 4.33 illustrates the obtained topologies for the "soft-kill" approach considering values of ΔT between -1 and 1.

Firstly, the topologies related to higher values of the temperature field (-10 K and 10 K) are not considered possible solutions since the optimization process diverges before the target volume is reached. Otherwise, the similarity between the results from both approaches, "hard-kill" and "soft-kill", becomes visible, mainly, for lower values of ΔT, where several similarities related to the material distribution can be observed. However, it is also noticeable that the "hard-kill" procedure produces more stable and feasible topologies, especially, when the temperature differential increases. Considering $\Delta T = 0.1$, Figure 4.34 represents the evolution of the objective-functions of both approaches and Figure 4.35 illustrates the evolution of the sensitivity number on element 31.

It is possible to notice less instabilities related to the "soft-kill" approach over the iterations. However, the required volume is reached at iteration 35 and, then, the problems tends to diverge immediately since there are no more possible solutions. Moreover,

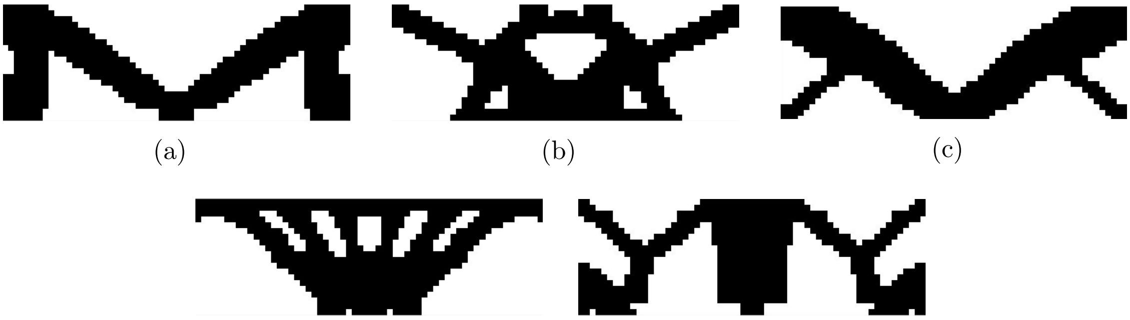

(a) (b) (c)

(d) (e)

Figure 4.33: Topologies produced considering a “soft-kill” approach for different values of ΔT: (a) $\Delta T = -1$ K, (b) $\Delta T = -0.5$ K, (c) $\Delta T = -0.1$ K, (d) $\Delta T = 0$ K, (e) $\Delta T =$ 0.1 K, (f) $\Delta T = 0.5$ K and (g) $\Delta T = 1$ K.

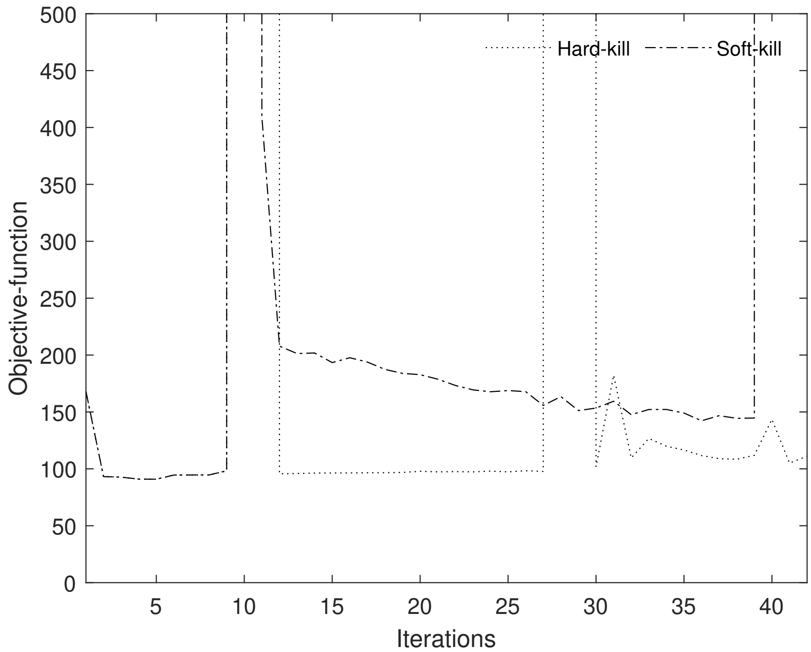

Figure 4.34: Evolution of the objective-function for the “hard-kill” and “soft-kill” approaches considering a structure under a uniform temperature variation equal to 0.1.

the objective-function assumes higher values over the optimization process and also, at the final solution, when compared to the “hard-kill” approach. Both approaches reach the target volume at iteration 35, being their behavior quite similar along the optimization process. Although the “soft-kill” approach establishes an almost constant sensitivity number over the iterations, at iteration 40, the problem diverges due to the non-existence of possible solutions. Nevertheless, it is possible to observe that the “soft-kill” approach presents a more stable objective-function until the target volume is achieved. However, the “hard-kill” approach produces better solutions, i.e lower values of the objective-function, and more defined and feasible topologies.

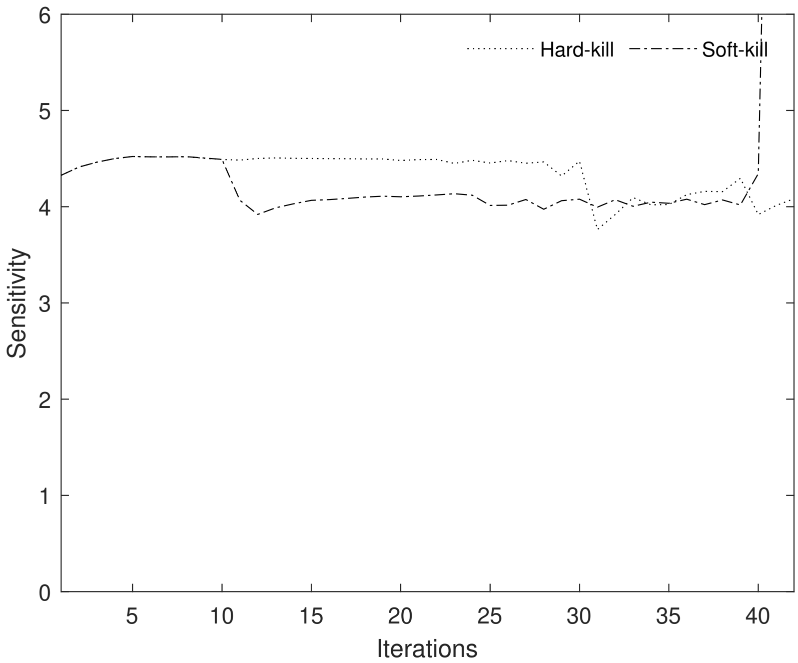

Figure 4.35: Evolution of the sensitivity on element 31 for the “hard-kill” and “soft-kill” approaches considering a structure under a uniform temperature variation equal to 0.1.

Chapter 5

Final remarks

5.1 Conclusions

The main challenge of this work was to study the instabilities associated with thermoelastic problems and introduce alternative strategies to control them. Thermoelastic problems are known for including boundary conditions that depend on the solution, namely, thermal loads. These are defined as design-dependent since their value depends on the material distribution on the structure. Therefore, they greatly affect the optimization process and, consequently, the obtained topologies.

In a preliminary phase, the structure of a Topology Optimization (TO) algorithm was studied and implemented considering different types of analyses. Initially, an elastic analysis was carried out to evaluate the structure's behavior when submitted to mechanical loading. Later, a thermal evaluation was performed taking into account the maximization of the structure's conductivity. By combining both objectives, a multi-objective approach was implemented. A global objective-function was established by weighting both objectives through a Pareto analysis. Different weights were assigned to each objective and, thereby, it was possible to study the influence of each analysis on the obtained topologies. Thereafter, the main challenge of this dissertation started by analyzing a structure's behavior when submitted to thermal loads. By prescribing a uniform temperature variation or by carrying out a thermal analysis, the structure was subjected to a temperature field. As introduced in section 2.3.5 and demonstrated in the results related to the thermoelastic analysis (*vd.* Sec. 4.3), the influence of thermal loads modifies the optimization process. Furthermore, their impact leads to the appearance of instabilities on the optimization process and, consequently, on the topologies. These instabilities translate into the existence of intermediate densities that are undesirable and in checkerboard problems, for example. Diverse works in the literature report similar problems related to these types of loads, however, only a few present alternative possibilities capable of solving them.

Thus, the main challenge consisted in trying to establish a strategy to control the stability of these problems. Therefore, it was implemented an alternative approach based on the Evolutionary Structural Optimization (ESO) method, known as Bi-directional ESO. The new procedure was carried out on a structure submitted to a uniform temperature variation. The obtained results allow to state that this procedure has the advantage of not having to deal with undesirable intermediate densities. Checkerboard problems were also avoided with the implementation of this method. Moreover, it was possible to conclude that a "hard-kill" approach was a more efficient procedure for this analysis when compared to a "soft-kill", being the obtained solutions more stable and topologically defined, resulting in better values of the objective-function. Furthermore, with regard to the Evolutionary Ratio (ER), a lower value establishes a more stable optimization process preventing the divergence of the problem due to the large changes applied to the topologies. However, a higher value of ER enables a faster convergence of the problem and, consequently, a faster optimization process.

Overall, the obtained results allow to state that a good decision was made regarding the alternative approach implemented to solve the mentioned issues. From a Finite Element Analysis (FEA) to topology optimization methodologies, the different procedures were carried out on benchmarks so the obtained results could be validated by comparing to the ones presented in the bibliography. Therefore, in order to obtain the presented results, all the methodologies described throughout this Dissertation were implemented on code. Thereby, as an outcome of this work, a computational tool capable of running the mentioned procedures was developed and validated. As mentioned, the background was set on GRIDS Alpha, a numerical simulation platform, based on the Finite Element Method (FEM), that was developed in academic environment. Its features were enhanced by the integration of the diverse functionalities that were developed in this work. The procedures related to FEM analysis and TO methodologies were implemented according to the modular concept of the original software and taking advantage of its FEM routines. The implementation of these methodologies on code allowed to gain a deeper knowledge on important details of optimization and FEM concepts. Also, the programming skills, very important in engineering, were improved. Lastly, it was possible to develop an user-friendly and open-source software in order to be a helpful tool for other students and, also, a platform to be further developed by them.

5.2 Future works

Considering the results presented throughout this Dissertation and since there are only a few works focused on efficient strategies to control the mentioned instabilities, it is important to improve the knowledge on this subject. Therefore, some guidelines for future developments are suggested:

- Extend the work developed to 3D, allowing to better model and simulate complex structures in a more realistic way;

- The implemented algorithms belong to gradient-based methods, even presenting different ways of computing the sensitivities. The application of stochastic algorithms, namely, metaheuristics methods, to thermoelastic problems is a possible work to develop in a near future. Although they are associated with a high computational cost, these do not require the evaluation of the objective-function's gradient so the issues related to the switch between signs of the sensitivity could be avoided;

- This work focuses on the existence of thermoelastic stress loads in topology optimization problems. However, there are another types of design-dependent loads, such as self-weight loading and centrifugal forces. These produce similar issues to thermal loads so a deeper knowledge on the subject is needed to solve the mentioned problems in a more efficient way;

- From the pedagogical standpoint, develop a user-interface that would allow students to try and test different optimization decisions on a given benchmark.

Intentionally blank page.

Bibliography

[A. Campos *et al.* 2015] A. A. Campos, J. Oliveira and J. Cruz. *Otimização Não-Linear em Engenharia: Cálculo Estrutural e Computacional Multiescala.* ETEP - Edições Técnicas e Profissionais, 2015.

[Ansola *et al.* 2006] R. Ansola, J. Canales and J. A. Tárrago. An efficient sensitivity computation strategy for the evolutionary structural optimization (ESO) of continuum structures subjected to self-weight loads. *Finite Elements in Analysis and Design*, 42(14-15):1220–1230, 2006.

[Arora 2017] J. S. Arora. *Introduction to Optimum Design.* Elsevier Academic Press, 4th edition, 2017.

[Bendsøe 1989] M. P. Bendsøe. Optimal shape design as a material distribution problem. *Structural Optimization*, 1(4):193–202, 1989.

[Bendsøe and Kikuchi 1988] M. P. Bendsøe and N. Kikuchi. Generating optimal topologies in structural design using a homogenization method. *Computer Methods in Applied Mechanics and Engineering*, 71(2):197–224, 1988.

[Bendsoe and Sigmund 2003] M. P. Bendsoe and O. Sigmund. *Topology Optimization: Theory, Methods and Applications.* Springer, Berlin, 2003.

[Bruyneel and Duysinx 2005] M. Bruyneel and P. Duysinx. Note on topology optimization of continuum structures including self-weight. *Structural and Multidisciplinary Optimization*, 29(4):245–256, 2005.

[Chen and Kikuchi 2001] B. C. Chen and N. Kikuchi. Topology optimization with design-dependent loads. *Finite elements in analysis and design*, 37(1):57–70, 2001.

[de Kruijf *et al.* 2007] N. de Kruijf, S. Zhou, Q. Li and Y. W. Mai. Topological design of structures and composite materials with multiobjectives. *International Journal of Solids and Structures*, 44(22-23):7092–7109, 2007.

[Deaton and Grandhi 2014] J. D. Deaton and R. V. Grandhi. A survey of structural and multidisciplinary continuum topology optimization: Post 2000. *Structural and Multidisciplinary Optimization*, 49(1):1–38, 2014.

[Deaton and Grandhi 2016] J. D. Deaton and R. V. Grandhi. Stress-based design of thermal structures via topology optimization. *Structural and Multidisciplinary Optimization*, 53(2):253–270, 2016.

[Deng and Suresh 2017] S. Deng and K. Suresh. Stress constrained thermo-elastic topology optimization with varying temperature fields via augmented topological sensitivity based level-set. *Structural and Multidisciplinary Optimization*, 56(6):1413–1427, 2017.

[Deng *et al.* 2014] S. Deng, K. Suresh and J. Joo. *Stress-constrained thermo-elastic topology optimization: A topological sensitivity approach.* In *Proceedings of the ASME Design Engineering Technical Conference*, Vol. 1A, Buffalo, New York, USA, August, 2014.

[Du and Olhoff 2004] J. Du and N. Olhoff. Topological optimization of continuum structures with design-dependent surface loading - Part I: New computational approach for 2D problems. *Structural and Multidisciplinary Optimization*, 27(3):151–165, 2004.

[Gao and Zhang 2010] T. Gao and W. Zhang. Topology optimization involving thermo-elastic stress loads. *Structural and Multidisciplinary Optimization*, 42(5):725–738, 2010.

[Hou *et al.* 2016] J. Hou, J. H. Zhu and Q. Li. On the topology optimization of elastic supporting structures under thermomechanical loads. *International Journal of Aerospace Engineering*, pp. 1–12, 2016.

[Huang and Xie 2007] X. Huang and Y. M. Xie. Convergent and mesh-independent solutions for the bi-directional evolutionary structural optimization method. *Finite Elements in Analysis and Design*, 43(14):1039–1049, 2007.

[Huang and Xie 2009] X. Huang and Y. M. Xie. Bi-directional evolutionary topology optimization of continuum structures with one or multiple materials. *Computational Mechanics*, 43(3):393–401, 2009.

[Huang and Xie 2010] X. Huang and Y. M. Xie. A further review of ESO type methods for topology optimization. *Structural and Multidisciplinary Optimization*, 41(5):671–683, 2010.

[Huang and Xie 2011] X. Huang and Y. M. Xie. Evolutionary topology optimization of continuum structures including design-dependent self-weight loads. *Finite Elements in Analysis and Design*, 47(8):942–948, 2011.

[Incropera *et al.* 2007] F. P. Incropera, D. P. DeWitt, T. L. Bergman and A. S. Lavine. *Fundamentals of Heat and Mass Transfer.* Jonh Wiley & Sons, New York, 6th edition, 2007.

[Kambampati *et al.* 2020] S. Kambampati, J. S. Gray and H. A. Kim. Level set topology optimization of structures under stress and temperature constraints. *Computers and Structures*, 235:106265, 2020.

[Kattan 2008] P. I. Kattan. *MATLAB Guide to Finite Elements: An Interactive Approach.* Springer, 2nd edition, 2008.

[Li *et al.* 1999] Qing Li, Grant P. Steven and Y. M. Xie. Displacement minimization of thermoelastic structures by evolutionary thickness design. *Computer Methods in Applied Mechanics and Engineering*, 179(3-4):361–378, 1999.

[Li *et al.* 2001a] Q. Li, G. P. Steven and Y. M. Xie. Thermoelastic topology optimization for problems with varying temperature fields. *Journal of Thermal Stresses*, 24(4):347–366, 2001.

[Li *et al.* 2001b] Qing Li, Grant P. Steven and Y. M. Xie. Thermoelastic topology optimization for problems with varying temperature fields. *Journal of Thermal Stresses*, 24(4):347–366, 2001.

[Li *et al.* 2010] D. Li, X. Zhang, Y. Guan and J. Zhan. *Topology optimization of thermo-mechanical continuum structure.* In *IEEE/ASME International Conference on Advanced Intelligent Mechatronics*, pp. 403–408, Montréal, Canada, July, 2010.

[Lourenço 2018] R. Lourenço. *Desenvolvimento de software modular para análise pelo Método dos Elementos Finitos em incompressibilidade.* Master's Thesis in Mechanical Engineering, Department of Mechanical Engineering, University of Aveiro, Aveiro, Portugal, 2018.

[Maxwell 1870] J. C. Maxwell. On Reciprocal Figures, Frames, and Diagrams of Forces. *Transactions of the Royal Society of Edinburgh*, 26(1):1–40, 1870.

[Michell 1904] A.G.M. Michell. The limits of economy of material in frame-structures. *Philosophical Magazine*, 8(47):589–597, 1904.

[Munk *et al.* 2015] D. J. Munk, G. A. Vio and G. P. Steven. Topology and shape optimization methods using evolutionary algorithms: a review. *Structural and Multidisciplinary Optimization*, 52(3):613–631, 2015.

[Oliveira 2013] J. Oliveira. *Metodologias de Optimização Topológica em Cálculo Estrutural.* Doctoral Dissertation in Mechanical Engineering, Department of Mechanical Engineering, University of Aveiro, Aveiro, Portugal, 2013.

[Pedersen and Pedersen 2010] P. Pedersen and N. L. Pedersen. Strength optimized designs of thermoelastic structures. *Structural and Multidisciplinary Optimization*, 42(5):681–691, 2010.

[Prager 1968] W. Prager. Optimality criteria in structural design. *Proceedings of the National Academy of Sciences of the United States of America*, 61(3):794–796, 1968.

[Querin *et al.* 1998] O. M. Querin, G. P. Steven and Y. M. Xie. Evolutionary structural optimisation (ESO) using a bidirectional algorithm. *Engineering Computations*, 15(8):1031–1048, 1998.

[Rao 2009] S. S. Rao. *Engineering Optimization: Theory and Practice.* Jonh Wiley & Sons, New Jersey, EUA, 4th edition, 2009.

[Rodrigues and Fernandes 1995] H. Rodrigues and P. Fernandes. A material based model for topology optimization of thermoelastic structures. *International Journal for Numerical Methods in Engineering*, 38(12):1951–1965, 1995.

[Rozvany 1998] G. I. N. Rozvany. Exact analytical solutions for some popular benchmark problems in topology optimization. *Structural Optimization*, 15(1):42–48, 1998.

[Rozvany 2009] G. I. N. Rozvany. A critical review of established methods of structural topology optimization. *Structural and Multidisciplinary Optimization*, 37(3):217–237, 2009.

[Rozvany *et al.* 1992] G. I. N. Rozvany, M. Zhou and T. Birker. Generalized shape optimization without homogenization. *Structural Optimization*, 4(3-4):250–252, 1992.

[Sigmund 2001] O. Sigmund. A 99 line topology optimization code written in matlab. *Structural and Multidisciplinary Optimization*, 21(2):120–127, 2001.

[Sigmund and Petersson 1998] O. Sigmund and J. Petersson. Numerical instabilities in topology optimization: A survey on procedures dealing with checkerboards, mesh-dependencies and local minima. *Structural Optimization*, 16(1):68–75, 1998.

[Sokół 2011] T. Sokół. A 99 line code for discretized Michell truss optimization written in Mathematica. *Structural and Multidisciplinary Optimization*, 43(2):181–190, 2011.

[Svanberg 2009] K. Svanberg. *Structural optimization.* In Encyclopedia of Optimization, C. A. Floudas and P. M. Pardalos (Eds.), pp. 3832–3834. Springer, Boston, Massachusetts, 2009.

[Teixeira-Dias *et al.* 2010] F. Teixeira-Dias, J. Pinho-da Cruz, R. A. Valente and R. J. Sousa. *Método dos elementos finitos - técnicas de simulação numérica em engenharia.* ETEP, 2010.

[Xia and Wang 2008] Q. Xia and M. Y. Wang. Topology optimization of thermoelastic structures using level set method. *Computational Mechanics*, 42(6):837–857, 2008.

[Xie and Steven 1993] Y.M. Xie and G.P. Steven. Technical note a simple approach to Structural Optimization. *Compurers & Structures*, 49(5):885–896, 1993.

[Yang *et al.* 2005] X. Y. Yang, Y. M. Xie and G. P. Steven. Evolutionary methods for topology optimisation of continuous structures with design dependent loads. *Computers and Structures*, 83(12-13):956–963, 2005.

[Zhang *et al.* 2014] W. Zhang, J. Yang, Y. Xu and T. Gao. Topology optimization of thermoelastic structures : mean compliance minimization or elastic strain energy minimization. *Struct Multidisc Optim*, 49:417–429, 2014.

[Zhu *et al.* 2019] X. Zhu, C. Zhao, X. Wang, Y. Zhou, P. Hu and Z. D. Ma. Temperature-constrained topology optimization of thermo-mechanical coupled problems. *Engineering Optimization*, 51(10):1687–1709, 2019.